



Cosmic Ray Project

APPLIED PHYSICS LABORATORY

A DIVISION OF THE DEPARTMENT OF PHYSICS
UNIVERSITY OF WASHINGTON

**Analysis of the Hard Component of the
Cosmic Radiation into its Protonic and
Mesonic Components at 3.4 Kilometers
and at Sea Level**

TECHNICAL REPORT

OFFICE OF NAVAL RESEARCH
CONTRACT N8ONR52008

**Parts of this document
are not reproducible**

APPLIED PHYSICS LABORATORY

UNIVERSITY OF WASHINGTON

A Division of the Department of Physics

ANALYSIS OF THE HARD COMPONENT OF THE COSMIC RADIATION
INTO ITS PROTONIC AND MESONIC COMPONENTS AT 3.4
KILOMETERS AND AT SEA LEVEL

By J. E. Henderson, C. E. Miller, D. S. Potter and
J. Todd Jr.*


TECHNICAL REPORT

OFFICE OF NAVY RESEARCH

CONTRACT N8onr 52008

Acknowledgment is made to the Bureau of Ordnance,
Navy Department for support of the early stages of
this research under Contract NOrd 7818.

Approved


J. E. Henderson, Director
Applied Physics Laboratory

*The physical material of this report was presented by J. Todd Jr.
as a dissertation in partial fulfillment of the requirements for the
Degree of Doctor of Philosophy of the Graduate School of the University
of Washington.

ACKNOWLEDGEMENT

The high altitude work described here was carried out on the grounds of the Climax Molybdenum Company at Fremont Pass in Colorado. The generous cooperation of C. S. Abrams, General Manager, and other personnel of this company is gratefully acknowledged. Important contributions to the research have also been made by Don Eng, electronic technician, and Elmer Wright, instrument maker, for our staff.

TABLE OF CONTENTS

	Page
LIST OF TABLES	111
Part	
I INTRODUCTION	1
Hard and Soft Components	4
The "N" Component	5
Ionization Chamber Studies	7
Cloud Chamber Studies	8
Counter Studies	9
Photographic Emulsion Studies	10
Momentum Distributions	13
Early Investigations of Protons	15
Recent Investigations of Protons	16
II EXPERIMENTAL METHOD	26
III THE EXPERIMENT	31
Procedure	33
Experimental Arrangement	33
Experiments Performed	35

TABLE OF CONTENTS (continued)

Part		Page
III (continued)		
	Equipment	36
	The Cloud Chamber	37
	The Magnets	38
	The Geiger Tubes	40
	The Electronics	41
	Illumination and Photography	45
IV	CURVATURE MEASUREMENT	46
	The Standard Curves	46
	Comparison Methods	47
V	DATA	48
VI	ERRORS AND CRITICISMS	62
VII	RESULTS	73
	Discussion of Momentum Distribution Found	73
	The Proton Spectrum	74
	The Meson Spectrum	77
	Mean Free Path in Lead	79
	Mean Free Path of "N" Component in the Atmosphere	80
VIII	COMPARISON WITH OTHER EXPERIMENTAL RESULTS	82
	Positive Excess	82
	Extension of M Correll's Result	82
	Comparison with the Results of Adams, Anderson, et Al	82

TABLE OF CONTENTS (continued)

Part	Page
VIII (continued)	
Comparison of Momentum Spectra	83
Comparison with the Results of Merkle and Goldwasser	83
Comparison with the Results of Hall	85
IX SUMMARY	88
BIBLIOGRAPHY	90

LIST OF TABLES

Table	Page
I Radii of Standard Curves	51
II Momentum Spectrum - Case A	52
III Momentum Spectrum - Case B	53
IV Momentum Spectrum - Case C	54
V Momentum Spectrum - Case D	55
VI Momentum Spectrum - Case E	56

ANALYSIS OF THE HARD COMPONENT OF THE COSMIC RADIATION
INTO ITS PROTONIC AND MESONIC COMPONENTS
AT 3.4 KILOMETERS AND AT SEA LEVEL

I

INTRODUCTION

Current interest in cosmic ray investigation is largely directed towards two general objectives. One is an interest in the phenomenon for itself and has for an end the explanation in cosmological terms of the origin of the radiation. The other, and perhaps wider interest, is to make use of the radiation to extend to very high energies our knowledge of nuclear phenomena. In the early periods of cosmic ray study (before 1930) the experimental techniques available measured only the total ionization produced by the radiation, both in the atmosphere and under various amounts of shielding material. Development of new techniques at about this time, principally those associated

with the use of Geiger counters, soon led to a phenomenological classification of the radiation into a hard and soft component. As techniques have become more quantitative, more discriminating classifications have become necessary. From the standpoint of nuclear physics it is appropriate to separate from the total radiation those particles which produce nuclear disruptions. Rossi (1) has called these particles the "N" component.

Many recent investigations of the interaction of this generalized nuclear component with the atmosphere and matter have been undertaken. The most common practice in these investigations is to study some particular phenomenon such as "bursts," "stars," "penetrating showers" or other type of reaction in order to infer the nature and behavior of the "N" component.

These studies usually cover a somewhat ill-defined range of energies and processes. Thus values for the absorption path length of the "N" component derived from these studies will vary widely, depending on the particular energy range or type of interaction emphasized by the experimental technique used. This situation will be improved only by the detailed study of the momentum distribution and intensity of each constituent of the "N" component.

Studies of the individual constituents of the "N" component have not been widely undertaken except for the

neutron constituent which is relatively easy to detect because of its unique properties. The high energy ionizing constituents of the "N" component, however, are exceedingly difficult to separate and most of the progress in this direction has been made in very recent years. The star producing characteristics of low energy pi-mesons was studied in detail by the use of photographic plates by the English physicists, particularly Occhialini and Powell in a series of papers running from 1946-1948. It has been shown from photographic plate studies that protons frequently cause nuclear disintegrations and, hence, are included in the "N" component, but no one had succeeded in separating mesons and protons with anything like quantitative results prior to 1948. In that year the investigation reported by Miller, Henderson, et al determined a lower limit for the proton flux in an extremely narrow momentum interval at 3.4 kilometers. The present paper described some measurements made in 1949 to 1950 which had the aim of determining the momentum spectrum of protons at 3.4 kilometers and also at sea level. The various techniques used in the study of the "N" component are discussed at length in order to compare the results obtained with those obtained in the present investigation.

Hard and Soft Components

For many years cosmic rays have been divided into two components which were labeled "hard" and "soft." The basis of separation is the respective range of the particles. The soft component is that portion which will not penetrate a layer of lead of 167 gm/cm^2 while the hard component will penetrate such a layer of lead. This division is justified by the behavior of sea level cosmic rays. If one considers the flux of cosmic rays below various layers of lead it will be found that the flux increases until a 3 centimeter layer of lead is reached, but as the layer becomes thicker the flux rapidly diminishes until a layer of 10 centimeters of lead has been reached. Further increases in the thickness of lead decrease the flux only slightly. The layer of 167 gm/cm^2 is designed to separate the rapidly absorbed soft component from the more penetrating hard component.

At sea level the conspicuous characteristic of the soft component is that most of the high energy particles in penetrating matter produce many lower energy particles. This is a characteristic of electrons and photons which are the principal constituent of the soft component at sea level. The processes involved in the multiplication are essentially electromagnetic in nature - Compton scattering, pair production, radiative processes due to electronic acceleration,

and knock on processes which are fairly well understood.

On the other hand the sea level hard component is essentially non-electronic in nature and its principal component is mesons. The separation into hard and soft components does not sharply distinguish mesons from electrons, for if the energy of the incident electron is high enough, there is a finite probability of at least one particle penetrating 167 gm/cm^2 of lead. Conversely, a meson having a momentum less than 300 Mev/c will not penetrate 167 gm/cm^2 .

The picture is further complicated by the presence of protons and neutrons particularly at higher altitudes. High energy protons lose energy by two strikingly different processes: first, by the gradual process of ionization, and secondly, by interaction with nuclei in catastrophic processes. At low energy ionization losses predominate but at high energies the nuclear interactions predominate. Neutrons lose energy principally by nuclear interaction, since they have no charge to cause Coulomb scattering. These properties will be discussed at greater length later.

The "N" Component

The separation into hard and soft components is not adequate for the purposes of this article so that other

criteria for separation must be used. One possibility is to separate the radiation into an electronic (cascade producing) and a non-electronic component. The electronic component includes electrons and photons. The non-electronic component contains mesons, protons, neutrons, V particles, and a variety of composite nuclei. The electronic component has been thoroughly studied and analyzed. The cascade process has been described mathematically by Bhabha and Heitler (2), by Carlson and Oppenheimer (3), and by Arley (4). A general review of electronic processes is given in Rossi and Greisen (5).

Except to make sure that electrons have been excluded from the measurements, the electronic component is of no interest in this paper.

Rossi (1) has designated those particles which cause nuclear disruptions or stars as a generalized nuclear component and has labeled them the "N" component.

Rossi (1) presents evidence which tends to show that electrons and photons cause relatively few stars, since the increase in the rate of stars with altitude is enormously greater than the increase of cascade showers. The same argument also applies to mu-mesons. The processes initiated by the "N" component are extremely varied and range from simple scattering phenomena through exchange collisions between neutrons and protons to complete nuclear disruptions.

These phenomena have been intensively studied in the last few years by many groups using an exceedingly diversified assortment of techniques. The actual processes occurring in nuclear interactions are not clearly understood but it is clear that when a direct collision occurs between an incident neutron or proton and a nucleus, that the nucleus may become disrupted and two to several particles may be ejected. The particles ejected may include protons, pi-mesons, electrons, neutrons, various nuclei, and "V" particles.

Ionization Chamber Studies

When the nuclear disruption occurs in an ionization chamber a large burst of ionization is detected; hence the name "burst" came into the literature. However, bursts include not only nuclear disruptions, but also dense air showers and at very high altitudes, single particles of high nuclear charge. The bursts due to air showers may be separated from single particles and nuclear disruptions by coincidence measurements between ionization chambers and Geiger counters. The occurrence of bursts has been studied by Bridge (6), Bridge, Hazen, Rossi and Williams (7), Bridge and Rossi (8), Hulsizer (9), McClure and Pomerantz (10). One of the latest burst studies has been conducted by G. N.

Whyte (11) at various latitudes and at altitudes to 100,000 feet. The results of these various experiments include a determination of a mean free path for the "N" component of 140 to 165 gm/cm² of air. In the upper atmosphere the path length increases to approximately 210 gm/cm².

Cloud Chamber Studies

Nuclear disruptions or "stars" have been studied in cloud chambers by many investigators, among the earlier studies being those of Neddermeyer and Anderson (12), Brode, Macpherson and Starr (13), and Fussell (14). Later researches have been made by W. M. Powell (15), W. E. Hazen (16), and by Fowler and Cool (17). These investigators have catalogued the stars by the number of prongs present, the penetrating power of the prongs, total energy, and similar data. They have found that the rate of star production can be fitted fairly well to the equation

$$R = R_0 e^{-\left(\frac{X}{L}\right)}$$

X = depth in atmosphere, L = a mean free path for removal when the "N" component, R₀, is an initial rate. At higher altitude this must be integrated over all directions to give a reasonable value and L must be modified to take account of the heavy nuclei in the primaries. At medium altitudes L is

found to vary depending on the size of star produced. Accepted values range from 120 to 165 gm/cm².

All of the cloud chamber studies have depended on the formation of stars in metallic plates except for one study by Valley (18) in a high pressure chamber for which detailed information has never been published.

Counter Studies

One of the interesting phenomena observed in a cloud chamber containing absorbing plates is the "penetrating shower" which originates at a point in one of the plates. A group of very penetrating particles occasionally occurs in a star and many of the particles will penetrate all of the remaining plates in the chamber. The angular spreading of the shower is often very small. Many studies (cf. Walker, Walker and Greisen (19)) have also been made of penetrating showers by means of Geiger-Mueller counters. Here again the rate may be fitted to an exponential function with respect to altitude and an absorption mean free path. It frequently happens that a shower has an electronic component and a more penetrating part, cf. ref. 19. The Cocconis and co-workers have published a large number of papers which deal with the occurrence of neutrons in penetrating showers.

Walker, Walker, and Greisen (19) have found that the absorption of the "N" component responsible for the production of penetrating showers has a mean free path in lead of 157 gm/cm^2 for charged particles and 165 gm/cm^2 for neutral particles. The mean free path in carbon was 80 and 82 gm/cm^2 respectively. These are higher than the values of the geometric cross section. The figure in lead is approximately that obtained by other workers, while that found for carbon is lower than some of the measurements of Cocconi and others.

Photographic Emulsion Studies

Stars have also been investigated in great detail by the use of photographic plates. Blau and Wambacher (20) probably conducted the first important investigation of stars with photographic plates. Among the most important of the early works using photographic plates is that of Stetter and Wambacher (21) who established the fact that the cosmic rays cause stars in emulsions, and also that there is a very rapid increase in the rate of star production as the altitude increases.

Later investigations have demonstrated the disintegration of pi-mesons into mu-mesons. Further investigations with photographic emulsions have disclosed many and varied nuclear interactions. Some of the various types include

incident low energy pi-mesons (mass, 275 electron masses) causing a nucleus to disintegrate emitting protons, alpha particles, heavier nuclei, occasional electrons, probably neutrons and possible gamma rays. Frequently a meson may be emitted. There have been occasions where an incident pi-meson has caused a nuclear explosion which emitted a secondary pi-meson which in turn caused a second nuclear explosion.

High energy incident protons cause nuclear explosions as do neutral particles (principally neutrons). If the incident particle has a very high energy it is probable that several so-called "grey" tracks will be formed which may be high energy mesons. The pencil so formed may be extremely narrow. Some examples are shown in the works of E. Pickup and Voyvodic (22), Camarini, Fowler, Lock, and Muirhead (23), and Lord, Feinberg, and Schein (24). It seems clear from these works that high energy mesons are formed in collisions involving extremely energetic (at least in the relativistic region) nucleons.

Blau and Wambacher (20) have found a direct proportionality between the number of slow protons and the rate of star production. If one makes the assumption, although it has no real logical basis, that this correspondence holds for protons of higher energies the same type of dependence on altitude should hold for protons as for stars. The

dependence of the intensity of the star producing agency on the depth of the atmosphere is

$$R = R_0 \int_0^{\frac{\pi}{2}} e^{-\frac{x}{L}} \sin \theta d\theta$$

by J. J. Lord (25)

where X is now the actual path traversed from the top of the atmosphere

R is the rate of star production

R_0 is the normalizing factor

L is the mean free path length

θ is the polar angle

At altitudes less than 60,000 feet this reduces to

$$R = R_0 e^{-\frac{X}{L}}$$

L varies from 120 to 165 gm/cm² for various kinds of stars. It will be seen later that the present investigation gives results which are in agreement with this equation. It should be carefully noted that the mean free path does not refer to the protons themselves but to the "N" component which causes stars.

It is interesting that neutron-produced stars reach a maximum intensity at an atmospheric pressure of 3.5 centimeters of mercury due to the lack of neutrons in the primary radiation.

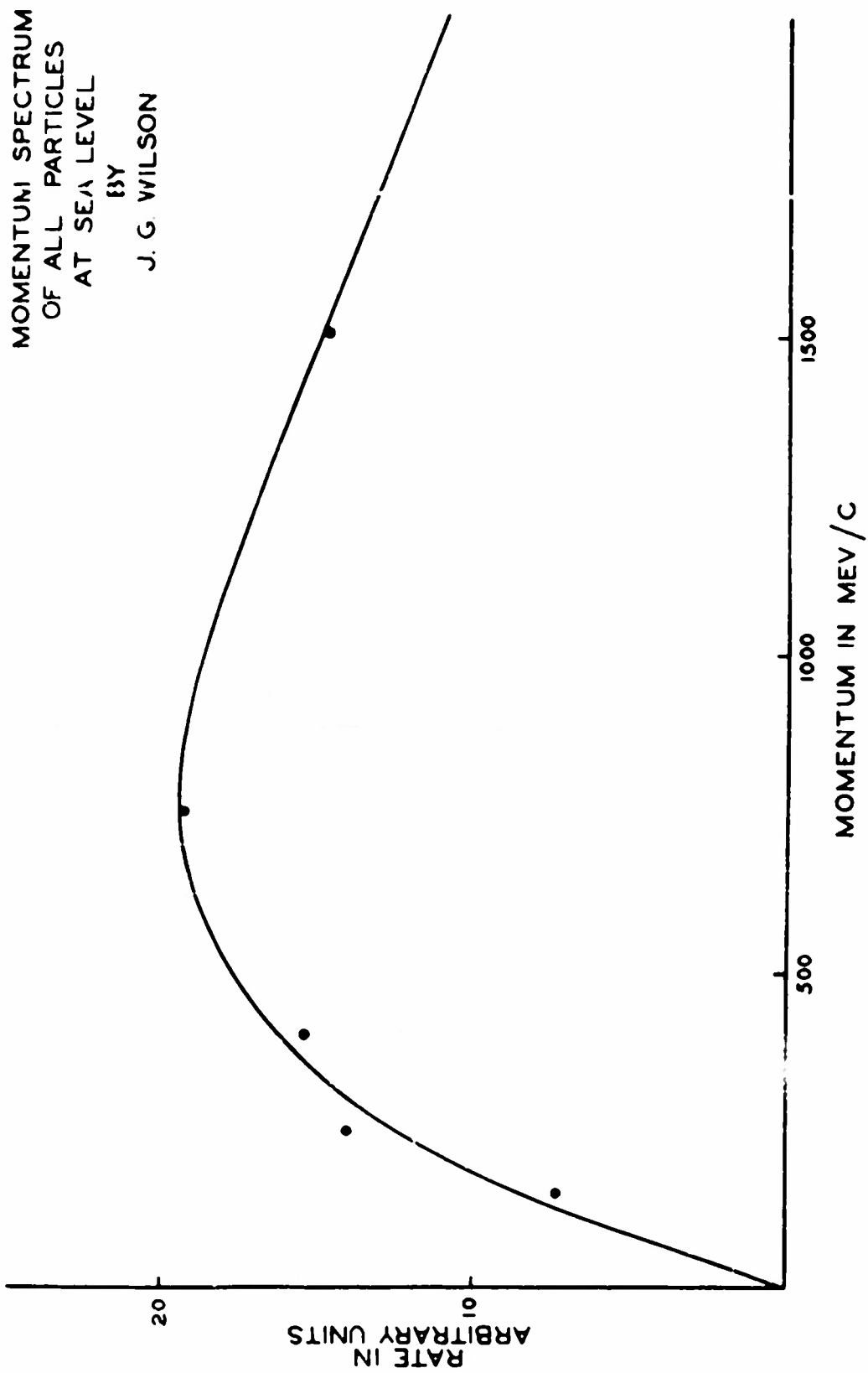
Momentum Distributions

The momentum distribution of the entire non-electronic component has been investigated by various physicists both at sea level and at higher altitudes. The earliest such measurement at high altitude was carried out by Neddermeyer and Anderson (12) in 1934, who determined the momentum distribution of all particles at 4.3 kilometers. They made observations on the ionization density and found that some 3 per cent of the cosmic radiation was heavily ionizing. In 1946 W. M. Powell (15) published the results of an extensive study of cosmic rays at 4.3 km using a combination of scattering and range to identify particles. He concluded that 3.3 per cent of the penetrating particles were protons.

As will be seen later, both of these estimates appear to have been low.

The momentum spectrum of the non-electronic component at sea level has been determined by means of cloud chambers by various investigators, notably Wilson (26), Hughes (to 10 Bev/C) (27), and Blackett (28) (to 20 Bev/C). The momentum spectrum of J. G. Wilson is reproduced in Fig. 1. The maximum of the curve lies at a value of 0.7 to 0.8 Bev/C.

A very recent and ingenious investigation has been carried out by Glaser, Hamermesh, and Safonov (29) who have determined the sea level momentum spectrum to the phenomenal value of 100 Bev/C.



The method used by these investigators was to place a strong magnetic field between two cloud chambers which were operated by a suitable Geiger tube telescope. They have found results in agreement with the researches mentioned above up to 20 Bev/C. Beyond this point the intensity continues to decrease.

Early Investigations of Protons

The investigation of the "N" component has been hampered by the difficulty of separating protons from mesons at higher momenta. The usual methods of separation in a cloud chamber involve the differing ionization densities for the same momentum, or the differing scattering properties, of mesons and protons. Both of these methods are applicable at comparatively low energies. Cloud chamber studies involving ionization densities are extremely laborious and probably somewhat uncertain because of the variation of the cloud chamber characteristics with time. Nonetheless, several such studies have been carried out at sea level (E. J. Williams (30), R. B. Brode, H. G. Macpherson and M. A. Starr (13)). Two studies worthy of note were carried out at 4300 meters by Neddermeyer and Anderson (12) and W. M. Powell (15). All of these studies found a very low percentage of protons in cosmic rays. The flux of very low

energy protons has been studied by means of photographic plates of Blau and Wambacher (20) and others.

The neutron intensity has been studied by many investigators who have determined the neutron flux at various altitudes using boron trifluoride counters and by use of recoil protons in photographic plates, and have obtained a certain amount of information regarding their energy distribution.

Recent Investigations of Protons

Recently several investigators have made researches which have at least partially separated the protonic component from the mesonic component. These include the investigations of Adams, Anderson et al at 30,000 feet (36), and the sea level researches of Merkle, Goldwasser, and Brode (31), Goldwasser and Merkle (32), Nonnemaker and Street (33). As all of these investigations apply to a greater or lesser extent to the problem at hand, they will be discussed at some length. The studies of Miller, Henderson et al (34) are the direct inspiration of the present work and will therefore be discussed extensively.

Another investigation which must be mentioned is that of Hall (35) who used a counter telescope to measure the integral range spectrum at 4350 meters. The principal interest in this paper is that the transformation to a

differential momentum spectrum leads to inconsistencies unless large numbers of protons are postulated.

Nonnemaker and Street, working at sea level, measured the momentum of particles which passed through a layer equivalent to 140 gm/cm^2 of lead and which stopped in a layer equivalent to 88 gm/cm^2 of lead. The means of measuring the momentum was a cloud chamber in a magnetic field of 4300 gauss. The identification of the particles was accomplished by means of the density of droplets along a track as compared to the density of droplets along a track of minimum ionization. Tracks occurring singly were classed as protons, mesons, or electrons; of 384 pictures, 227 were mu-mesons, 10 were dense tracks having momentum greater than 250 Mev/c, 23 were energetic particles which did not trigger the anticoincidence tray, 15 were electrons with momenta less than 70 Mev/c, and 73 were other electronic events.

They obtained a positive excess for the mesons of $.94 \pm .07$.

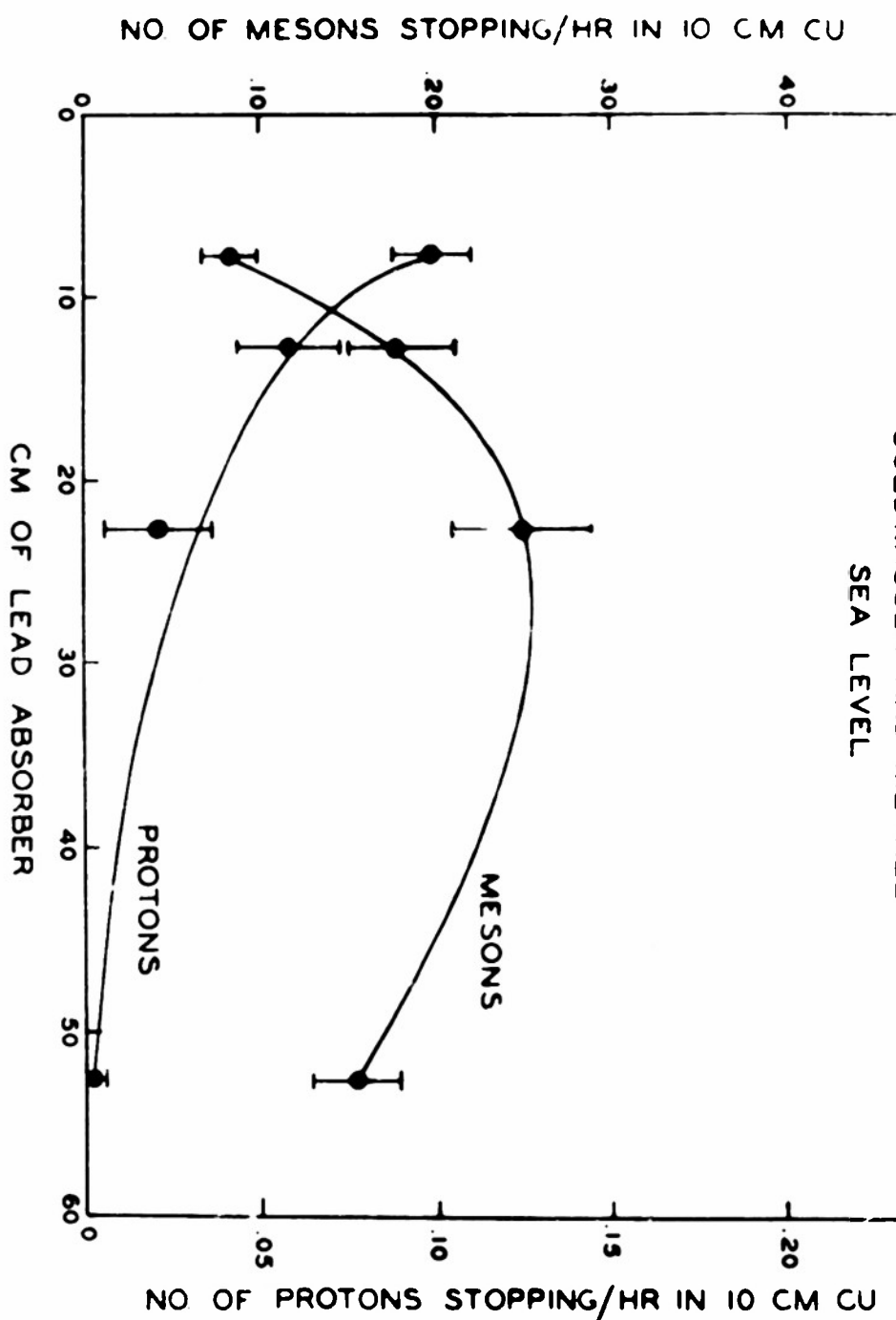
Nonnemaker and Street have conducted their research from the standpoint of mass determinations and consequently have conducted the experiment from a viewpoint which makes impossible an easy interpretation of the data with respect to the analysis into various components. In the first place, the amount of absorber over the chamber is nearly a mean free path length for energetic protons, hence nearly 60 per cent

of the very energetic protons in the atmosphere are lost in the absorber. Secondly, the absorption of protons due to ionization loss is complete up to a momentum of 750 Mev/c. That they obtained any protons at all is undoubtedly due to the production of protons in the lead absorber above the chamber.

Merkle, Goldwasser, and Brode (31) conducted an experiment in which simultaneous momentum and range measurements were made at sea level for the purpose of obtaining mass measurements. This experiment showed a protonic component of about 1 per cent of the total penetrating component. These authors found that as many protons as mesons stop in the range 4-13 centimeters of lead.

Goldwasser and Merkle (33) have extended these measurements with results substantially differing from those of other investigators. They find considerably more protons stopping between 4 and 13 centimeters of lead than mesons. Although they find a mean free path for absorption of 12 centimeters for lead placed above the cloud chamber, they find a mean free path of 4 centimeters for lead in the range measuring chamber. The differential range spectra for mesons and protons found by these authors is reproduced in Fig. 2. A comparison of these results with those of the present investigation will be made later.

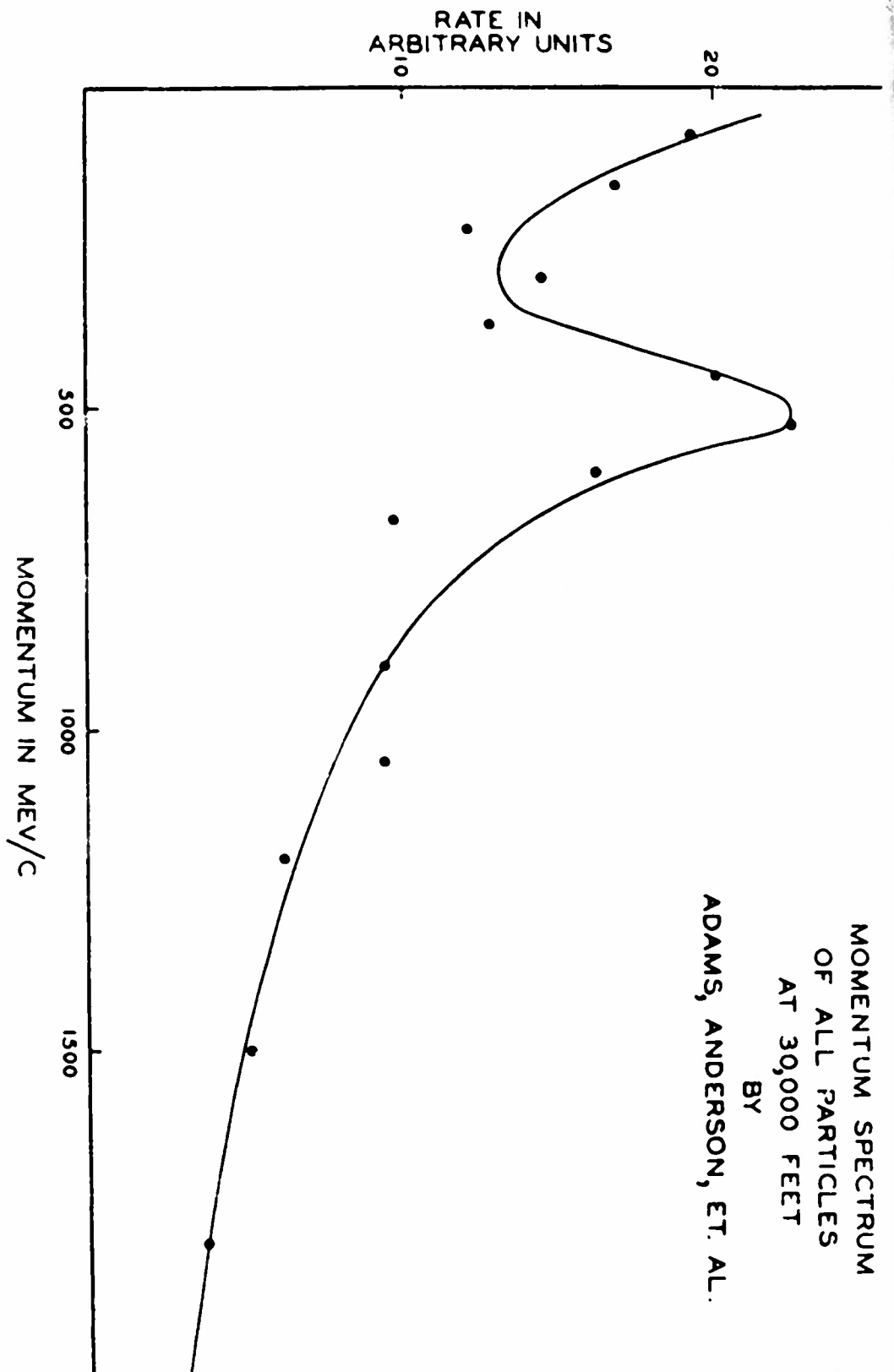
DIFFERENTIAL RANGE SPECTRA FOR PROTONS AND MESONS -
 MODERATOR ABOVE APPARATUS
 GOLDWASSER AND MERKLE
 SEA LEVEL



Probably the first of the recent investigations which indicated the presence of large numbers of protons in cosmic rays is that of Adams, Anderson, et al (36) who obtained a momentum spectrum at 30,000 feet by flying a magnetic cloud chamber in a B-29. The momentum distribution obtained (which is shown in Fig. 3) is featured by a very high peak at a momentum of about 500 Mev/c. There was a 3-1/2 centimeter brass casting between the sensitive volume of the chamber and the lower coincidence tube. As the peak was due entirely to positive particles and occurs at a momentum which is just at the absorption cutoff for protons traversing the brass casting, it is highly probable that the peak is due to a very large number of protons in the radiation. The statistics are not sufficient to permit a satisfactory estimate of the protonic flux, but the evidence points to a very large number of protons compared to previous estimates.

Hall (35), in transforming the integral range spectrum which he obtained at 4.3 kilometers into a differential momentum spectrum used the hypothesis that all particles observed were mesons. The momentum spectrum obtained had a tremendous peak at about 250 Mev/c. Hall realized that the distribution of this type would be extremely unstable with respect to altitude and if there were only mesons in the radiation that this spectrum required a tremendous generation of mesons at this altitude. More recent theoretical

MOMENTUM SPECTRUM
OF ALL PARTICLES
AT 30,000 FEET
BY
ADAMS, ANDERSON, ET. AL.



and experimental work has shown that mesons are created as a result of collisions between nucleons which he hypothesized were not present.

Since the present work permits the estimation of the number of protons at 3.4 kilometers, some correlation with Hall's differential momentum spectrum should be possible as there are only about 85 gm/cm^2 of air between these altitudes. This will be discussed further on.

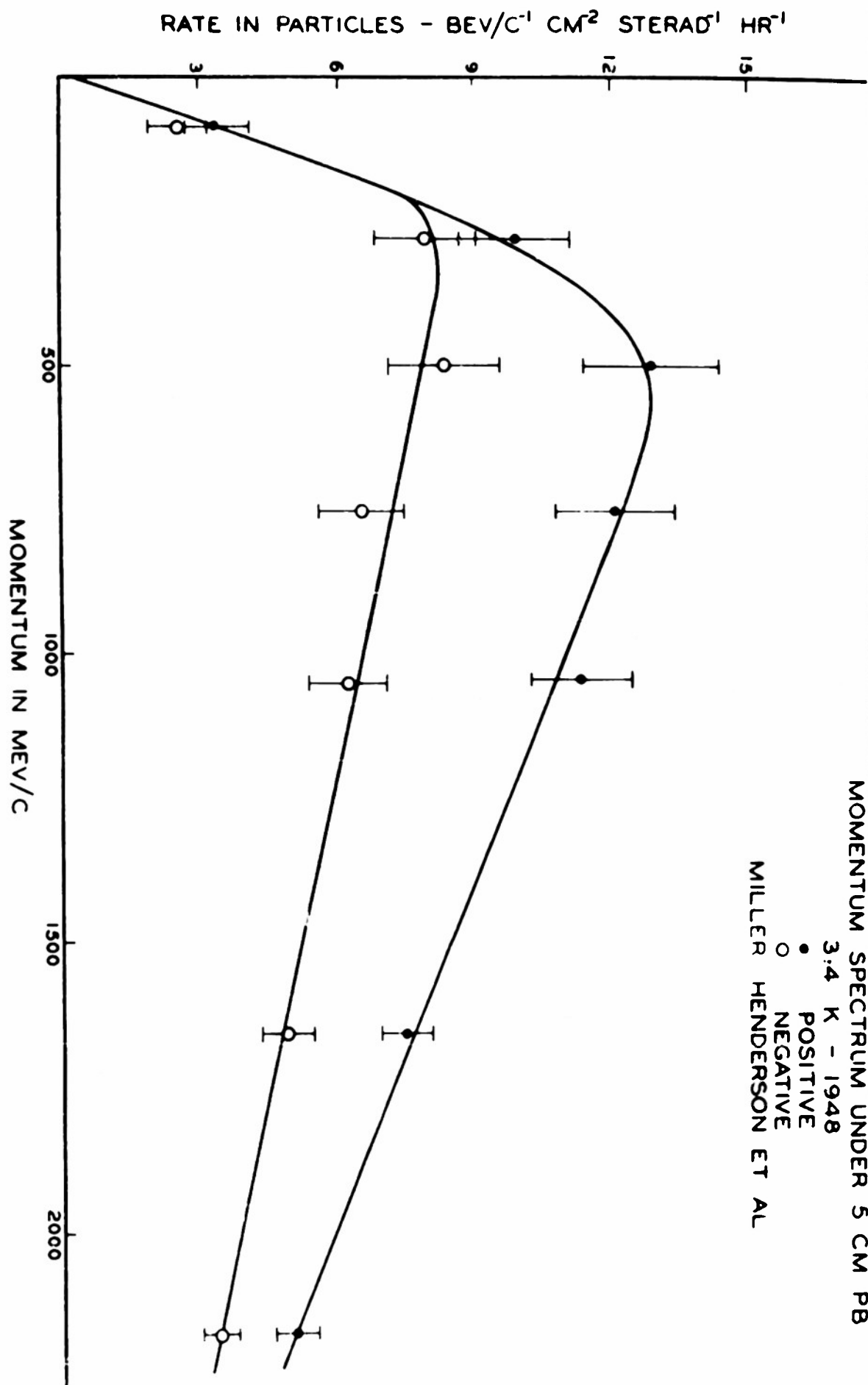
Another recent work which indicated the presence of a significant number of protons in cosmic rays at 3.4 kilometers is the work of Miller, Henderson, et al (34) who measured the momentum spectrum of cosmic rays under various thicknesses of lead. The spectrum under 5 centimeters of lead is shown in Fig. 4. During the examination of the data it was noted that some of the tracks of particles having relatively high momenta showed an ionization that was several times minimum, although mesons with such momenta would have produced tracks of almost minimum ionization. All but three of these tracks showed curvatures denoting positive charge if the particles were traveling downwards.

A momentum plot of all of these heavily ionizing particles showed a low momentum cutoff which corresponded to the momentum which a proton must have in order to get from the cloud chamber into the sensitive volume of the lower Geiger counter. In view of these facts, it is

MOMENTUM SPECTRUM UNDER 5 CM PB

3.4 K - 1948

• POSITIVE
○ NEGATIVE
MILLER HENDERSON ET AL



probable that these particles were protons. It was found that they constituted some 10 per cent of the singly occurring ionizing part of the non-electronic component at a momentum near 500 Mev/c.

The judgment of the ionization of the track was somewhat subjective. That is, a series of frames was examined simultaneously and if one of the tracks appeared particularly heavy, in the opinion of the person examining it, it was recorded as a heavy track. Several items contributed to the uncertainty of the identification. In the first place, the chamber was counter-controlled so that the intervals between expansions was random except for a 1-1/2 minute chamber recovery time.

In the second place, the time delay between the detection of the particle and the expansion of the cloud chamber was so short that the droplets did not have time to completely form or the ions to diffuse away from each other, so that actual counting of droplets to determine ionization accurately was entirely unfeasible. In addition there were sometimes slight variations in illumination. It was felt that the estimate given was a lower limit of the protons and that many more protons actually existed in the radiation.

The previous work on the "B" component has been given in detail above. The information available about protons was very limited, consisting of knowledge that protons

existed in fairly large numbers. No proton momentum spectrum had been published. The present investigation permitted a quantitative description of the momentum distribution of protons in the momentum interval from 500 Mev/c to 2 Bev/c. As an important by-product of this research an estimate of the mean free path for absorption due to nuclear reaction has been made possible.

Subtraction of the proton momentum spectrum from the momentum spectrum of the non-electronic component found by Miller, Henderson, et al (34) permits an approximation of the meson spectrum.

II

EXPERIMENTAL METHOD

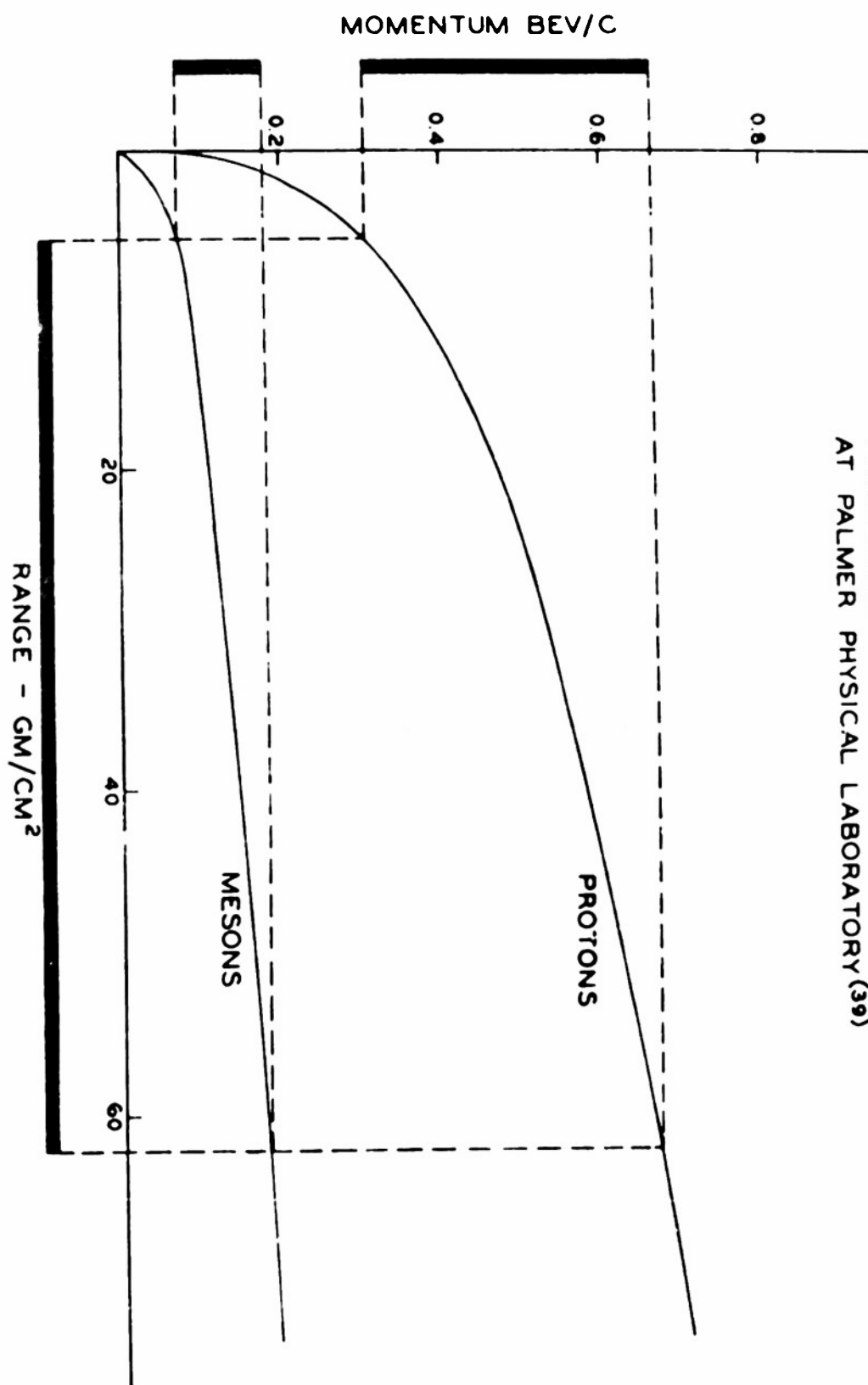
The search for a method of distinguishing protons that does not involve a subjective treatment and which permits the determination of their momentum spectrum always necessitates the choice of two techniques. The determination of the momentum spectrum is a measurement for which the magnetic cloud chamber is uniquely fitted. There is no other tool which is nearly so effective for momentum measurements or which even measures the momentum directly. Since it is desirable to avoid any possible ambiguity, the first necessary choice is the magnetic cloud chamber. This leaves one other property to be measured. The properties which are used frequently for this type of study are the scattering, ionization density, and range of the particle. The scattering properties did not seem capable of giving accurate enough information in the small chamber available since no lead plates could be introduced because they would shorten the length of track available for curvature measurements to the point where no accuracy could be obtained. Ionization measurements suffer from similar defects. In order to measure ionization accurately, it is necessary to delay the expansion of the chamber until considerable diffusion has occurred in the track. It is then impossible to

measure the curvature of the resulting broad, diffuse track with any degree of accuracy. In any case the ionization density method is limited to low energies.

The one remaining possibility was a simultaneous measurement of momentum and range. The difficulties that arise here are fortunately not serious. In the first place the measurements do not mutually interfere so that the accuracy of either can be carried out to the limit of the equipment without bothering the other. In the second place the range of a particle is a rapidly varying function of momentum so that for particles of momenta considered in this experiment the range is suitable parameter for the determination of particle characteristics. As a counter telescope appeared to be considerably more flexible than a range cloud chamber, this was the method used.

The principle of separation of protons from mesons can be shown most easily by reference to Fig. 5. It is based on the vast differences of the range-momentum relations of protons and mesons. Fig. 5 shows the range-momentum curves for mesons and protons. The heavy horizontal bar marks the range interval 0.5 to 5.5 centimeters of lead. The short vertical bar represents the momentum interval for which mesons would stop in this range. Similarly the long vertical bar marks the momentum range for which protons would have this same range. If there were no scattering

RANGE MOMENTUM RELATIONS FOR PROTONS AND MESONS
 FROM DATA PREPARED BY E. P. GROSS
 AT PALMER PHYSICAL LABORATORY (39)



and the anticoincidence tray were 100 per cent efficient the momentum spectrum obtained would be two peaks, that with lower momentum being due to mesons and that with higher momentum due to protons, with vertical cutoffs. The picture is complicated by the small angle scattering to which the particles are subjected and also by catastrophic losses of protons. A glance at Fig. 9 shows the momentum spectrum obtained for those particles which stop in 0.5 to 5.5 centimeters of lead. The extremely clear separation of the two peaks shows the efficacy of the method.

If ionization losses alone were of significance, the information derivable from this series of measurements would be limited to a momentum of about 1.2 Bev/C for protons. However, as we have already seen, the "N" component is absorbed in lead by nuclear interaction with an absorption mean free path of 156-165 gm/cm². Since protons are certainly one constituent of the "N" component they also must be absorbed with a mean free path of about 160 gm/cm². On the basis of this figure which is not philosophically justified in a 5-centimeter absorber about one third of the high energy protons are stopped while at 10 centimeters the fraction is about 55 per cent of the total protonic flux. Thus from the data found in this experiment it is possible to get a fair approximation of the number of protons in the cosmic radiation. Although due to scattering difficulties

and the need to add several partial spectra the probable error is large at high energies. A crude estimation of the mean free path of protons (as distinguished from the generalized "N" component) in lead can be made from the number of protons stopped in varying amounts of lead, but the probable error is large, due to the method necessary to get the proton flux at higher momenta. This figure may then be used to calculate the total protonic flux.

This experiment differs markedly from that reported by Miller, Henderson, et al (34) because the experiment that these investigators performed was a simple momentum measurement of all particles which had a sufficient range to penetrate the moderating lead above the cloud chamber. The information obtained about protons was due entirely to the heavy ionization of these particles. Estimates of proton intensity were limited to a narrow momentum band and served only to set a lower limit to the intensity in this band.

III

THE EXPERIMENT

The expedition of 1948 had found that the use of the facilities provided by the Climax Molybdenum Company greatly simplified the problems of the expedition. It was therefore decided that the present data should be obtained by Climax. A 22-foot van-trailer with an International semi-tractor for locomotion was obtained and fitted out for the use of the expedition. A small dark room was built into the trailer and served for the processing of much of the film. On-the-spot analysis of sufficient film to indicate the trend of the experiment greatly facilitated the experimental procedure. Perhaps the greatest handicap to the experiment was the extremes of temperature encountered within the truck.

The motor generator set was installed on a Navy 6X6 truck and covered with an aluminum roof. These two trucks plus a small Dodge truck were taken to Climax, Colorado (altitude 3.4 km) on the first of September 1949. Climax measurements were carried out in September, October, November, and early December, after which the trucks returned to Seattle in a blizzard. Fig. 6 shows the trucks on location at Climax.

The Seattle measurements were obtained in May and June 1950.

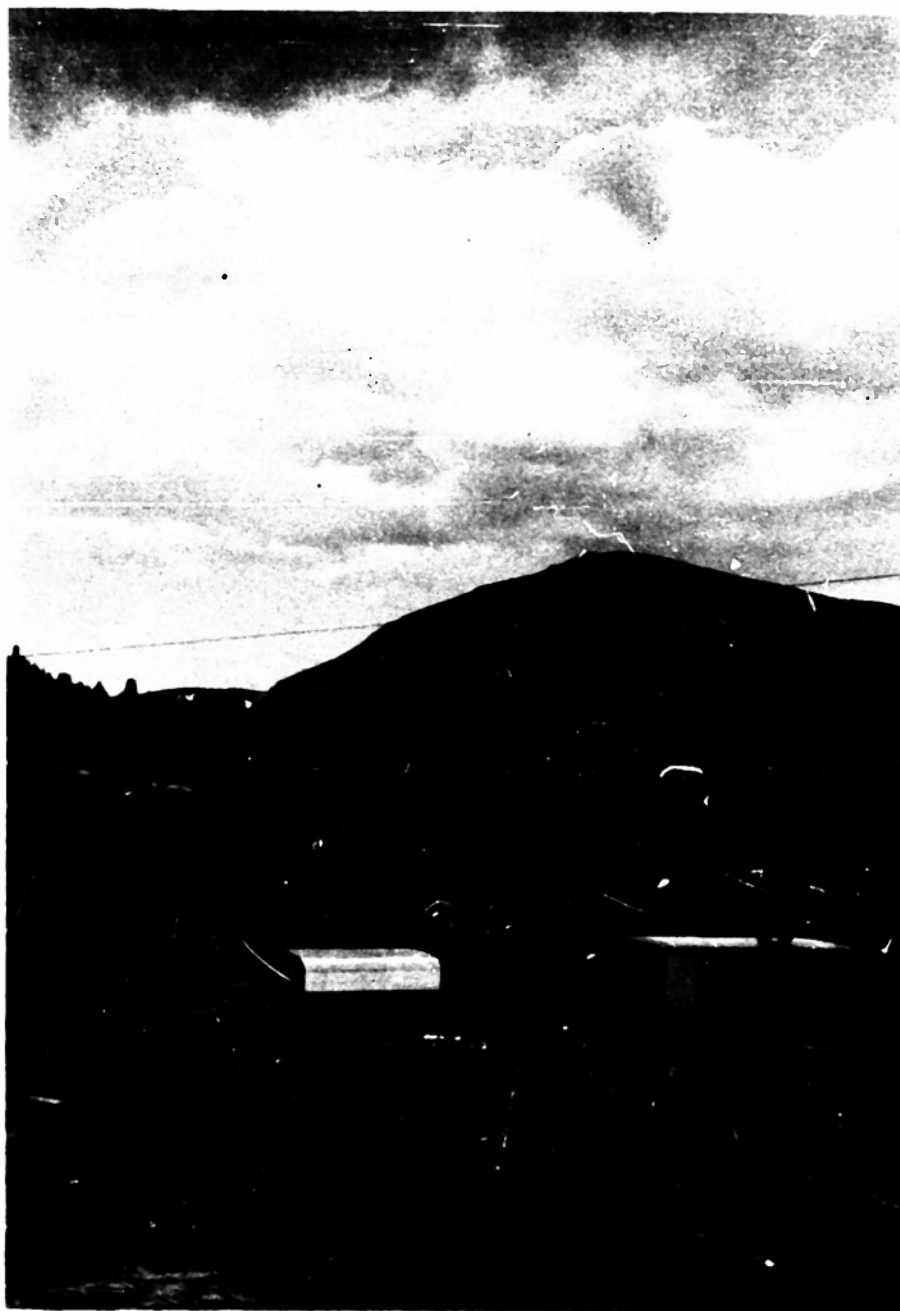


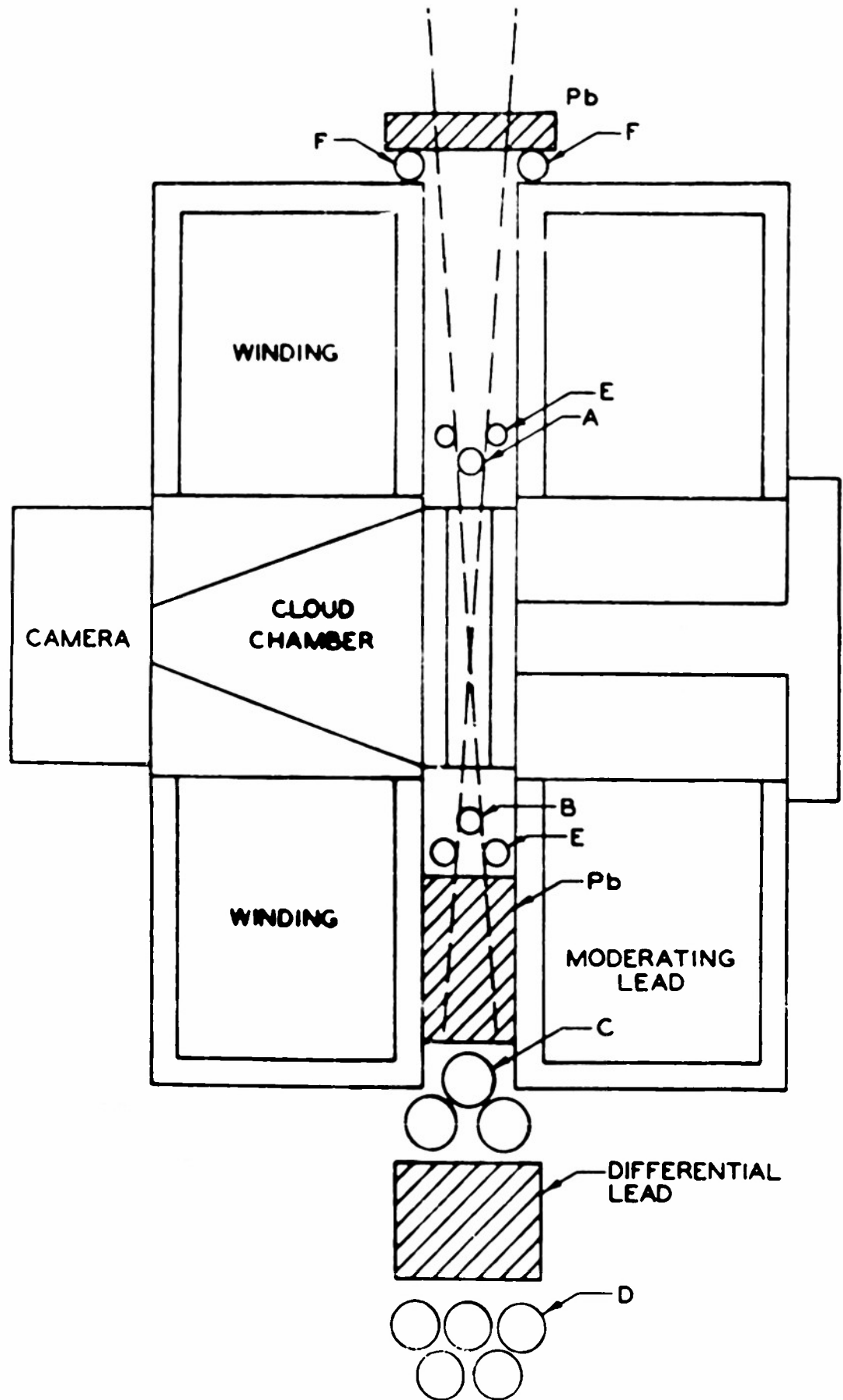
FIGURE 6. TRUCKS ON LOCATION AT CLIMAX

Procedure

Experimental Arrangement

The experimental arrangement shown in Fig. 7 was used. Counters A, B, and C are in coincidence while the counters at D and E are in anticoincidence. The counters at E were placed in anticoincidence for the purpose of reducing the number of shower pictures obtained since only singly occurring tracks were of importance in this study. It is apparent that only those particles with sufficient range to penetrate the lower wall of the cloud chamber and the material between it and tray C, but of insufficient range to trigger one of the counters at D will be photographed. The minimum material between the sensitive volume of the cloud chamber and the Geiger tube was equivalent to 0.5 centimeters of lead, which provided a convenient minimum absorber for the purpose of separating mesons from protons.

Since the experiment was designed to separate protons having various momenta (following the principle illustrated in Fig. 5) it was necessary to obtain particles with varying ranges. The moderating lead set the minimum range, counter C acting as a recording mechanism to indicate that the particle had actually penetrated the lead. Counter D then eliminated all particles having sufficient range to penetrate



both the moderating and differential lead. The momenta of only those particles stopping in the differential lead were measured.

Experiments Performed

Three series of measurements using this experimental arrangement were made at Climax, Colorado (altitude 3.4 kilometers) during the summer and fall of 1949. These will be referred to as Cases A, B, and C. The only difference in the series is in the amounts of moderating and differential lead (indicated in Fig. 7). The amount of lead in the three cases is shown in the following table:

Case	A	B	C
Differential Lead	5 cm	10 cm	10 cm
Moderating Lead	0	5	15

In addition to the moderating absorber deliberately introduced there was sufficient material to be equivalent to an additional half centimeter of lead between the sensitive volumes of the cloud chamber and Geiger tube C.

Two additional series of observations were made at sea level using an anticoincidence tray at D that was redesigned to increase its efficiency. This will be discussed later in this report. No moderating lead was used in either series. The first of these series (Case D) was a repetition

at sea level of Case A. The second, made because of the extremely low intensity of protons at sea level used 10 centimeters of differential lead

Case	D	E
Differential Lead	5 cm	10 cm
Moderating Lead	0	0

Equipment

Due to the extremely varied and complex nature of the equipment used in this investigation, the discussion of the apparatus will be divided into the following sections:

1. The cloud chamber
2. The magnets
3. The Geiger tubes
4. The electronics
5. Equipment for analyzing the data

Each of these divisions will be discussed in considerable detail. A description of the experimental arrangement as set up for use has been given previously. Most of the component parts of the equipment have been described elsewhere (34, 37).

The Cloud Chamber

The cloud chamber is basically a diaphragm type. The design of the chamber is unique in that the expansion chamber is connected to the sensitive volume by a 2 x 10 inch brass tube. This was done so that the distance between magnet poles could be kept as small as possible. The expansion chamber and the sensitive volume are each of fairly standard design. The connecting tube introduced special problems since the assembly acted like a Helmholtz oscillator causing local overexpansions which prevented normal operation. The technique which cured this effect was to stuff the tube loosely with copper wool. The copper wool offered enough additional damping so that any remaining oscillations were so small that they did not give overexpansions.

Tracks formed sufficiently within .02 seconds after the initiation of the expansion to permit successful photographing of them. After .05 seconds delay, the tracks were sufficiently dense so that accurate curvature measurements could be made. Tracks were extremely narrow, being only .7 millimeters wide. Satisfactory momentum measurements to a momentum of 2-1/2 Bev/C could be made.

The cloud chamber was filled with an excess of a mixture of 60 per cent normal propyl alcohol and 40 per cent water as a condensing agent, the permanent gas being argon at a gauge pressure of 1.3 atmospheres. Compression of the

cloud chamber was accomplished by use of backing air at a pressure of 1.7 atmospheres held by means of a magnetically activated pop valve which was designed with fast operation as the principal criterion (the moving parts were held to minimum weights). Expansion was accomplished by voiding the backing air into the atmosphere. A capillary was provided in the air supply so that only a small amount of air would flow during the expansion cycle. Measurements have indicated that the expansion was essentially complete within .01 second after the detection of a desired event.

The Magnets

The magnets are wound from 0.25 x 0.80 inch copper strip and are contained in steel housings, which with the steel cores form the magnetic circuits. The magnet, independent of the supporting framework, weighs about 2000 pounds; approximately half of this weight is steel and half is copper. When operating at a field strength of 8200 Gauss, the magnet requires a current of 800 amperes, giving a total of 1.9×10^5 ampere turns. Power dissipation under these conditions is 25 kilowatts. The original calibration of the field was made by means of a flip coil mounted on the axis of the magnets. Exploration of the field uniformity was made using a bismuth spiral and Schmidt bridge. Errors due to non-uniformity of the field were negligible as the field

varied less than 1 per cent throughout the illuminated region of the chamber.

Cooling of the magnets was effected by means of rapidly circulating oil through a system of baffles that insured a flow of oil over every surface of the buss. The oil, flowing at a rate of 60 gallons a minute, was cooled in a heat exchanger with water being the ultimate agency for carrying away the heat generated in the magnets.

The temperature was controlled by means of a by-pass valve which permitted a fraction of the oil to circulate without passing through the heat exchanger. The by-pass valve was controlled by a small two-phase motor operated by a Brown potentiometer amplifier which was activated by the signal from a Wheatstone bridge, one arm of which was 110 ohm non-inductive coil wound of No. 40 copper wire immersed in the oil stream at the intake to the magnet cooling system. The temperature of the cooling oil flowing into the magnets was constant to 0.01 degrees Centigrade. Since the temperature control of the input oil was so constant, the cloud chamber was placed in good thermal contact with the magnet core, resulting in extreme constancy in the cloud chamber temperature.

The D.C. current was obtained from a motor generator set that furnished 800 amperes at 28 volts. The cooling water, supplied by the Climax Molybdenum Company, was at a

uniformly low temperature and was a contributing factor to the fine results obtained.

The Geiger Tubes

The Geiger tubes were all of glass wall type. An oxidized copper cathode and 5 mil tungsten anode were used in all of the tubes. Four sizes of tubes were made, sensitive volumes of these tubes being $3/4 \times 6$ inches, $1-1/4 \times 12$ inches, $1-1/4 \times 18$ inches, and $1-1/4 \times 24$ inches. Springs were placed in the longer tubes in order to take up the slack when the central wires were flashed. The tubes were filled with a mixture of 10 per cent petroleum ether and 90 per cent argon to a pressure which gave an operating voltage of 1325 volts (about 12-15 centimeters of mercury). The counting rate was constant within 5 per cent over the 300-volt plateau.

These tubes were all baked out several hours at about 500°C under a vacuum of 10^{-3} mm. The central tungsten wires were heated to a bright orange by an electric current for half an hour and then flashed a brilliant white for a few seconds. The copper was oxidized by permitting air to enter the tube while it was still hot. Apparently the exact amount of oxide was not critical and could be varied from an almost invisible layer of the red oxide Cu_2O to a fairly heavy brown layer which probably contained some CuO . The

tubes which failed because of overvoltage or old age could usually be revived by pumping out, reflashng the wire and refilling. The efficiency of the Geiger tubes was found to be over 99 per cent and the 1-1/4 inch tubes had an approximate life of 10^8 counts.

Four channels of anticoincidence tubes were provided so that the dead time of the anticoincidence tray was reduced to a minimum. This comes about as follows. When a Geiger tube fires, the voltage across the tube falls below the lower level of the Geiger plateau for a period of 100-200 microseconds. During this interval all of the Geiger tubes connected in parallel with the triggered tube are inoperative. In order to minimize errors of inclusion due to a particle passing through one of the inoperative Geiger tubes the number of tubes in any one group was kept low so that the largest possible number of tubes was in operation at all times. Errors from this source were of the order of 1 per cent.

The Electronics

The electronic circuits may be divided into four parts: an event selector, a cloud chamber control, a program unit, and an auxiliary high voltage flasher supply.

Event Selector. The event selector, as the name implies, chooses an event which triggers the proper Geiger

tubes in the coincidence train and fails to trigger any tubes in the anticoincidence train. The Rossi type coincidence circuit has three channels which may be switched so that a coincidence will be registered if simultaneous (within the 1.6 microsecond resolving time of the unit) pulses are received on 1, 2, or 3 channels. The output of the Rossi tube is fed into a univibrator which delays the pulse two microseconds and provides a 1.6 microsecond square wave output. This pulse is fed into a mixer tube and at the same time initiates circuits which record the coincidence. The output of the coincidence and anticoincidence pulse shapers are fed into a selector switch which permits selection of any of the coincidence or anticoincidence channels or the sum of all four anticoincidence channels for the purposes of scaling the tubes. This function is necessary because it permits the condition of the Geiger tubes to be determined.

The anticoincidence pulses are amplified and mixed. After being shaped the anticoincidence pulse is fed into an anticoincidence pulse generator which furnishes a 5 microsecond blanking pulse.

The output of the Rossi coincidence tube and the anticoincidence pulse generator are fed into a mixer tube. If no anticoincidence pulse is present the mixer output is fed to the program unit.

If there is a simultaneous coincidence and anticoincidence pulse, the coincidence pulse arrives two microseconds after the anticoincidence pulse and lasts only 1.6 microseconds. Thus the blanking pulse completely blankets the coincidence pulse.

Cloud Chamber Control Unit. The cloud chamber control unit performs the following services upon receipt of a signal from the program unit:

1. Expands the chamber
2. Turns off the clearing field
3. Actuates the flash lamps, after a suitable time delay
4. Rewinds the camera
5. Records the expansion
6. Turns on the clearing field
7. Recompresses the chamber
8. Provides a time delay for the cloud chamber to recover

Time delays of the order of 4 seconds or less are provided by univibrators. The 1-1/2 minute sterilization delay is provided by a timing motor. The photo flash timer is varied by changing the capacitance of an R-C timer in a binary system so that any delay between .0 second and .16 second in steps of .01 second may be obtained by a proper manipulation of the four on-off switches.

The Program Unit. The program unit provides for operation of two separate cloud chambers as desired from either of two event selector units and it also permits the interconnection of the two units.

In addition to the programming of the chamber control units this chassis carries the registers for recording the number of coincidences and coincidence minus anticoincidence from each event selector. A binary scale of 16 is included for the purpose of scaling the Geiger tubes on each of the channels. A Geiger voltage supply capable of furnishing 1600 volts, but which is limited to about 1450 volts for the protection of the Geiger tubes was constructed by using a small radio frequency oscillator and tank circuit.

The binary scales are of extreme interest since they are completely stable, trouble free, and manufactured in packaged units with no tailoring necessary. The units were manufactured with the idea that if one failed it would be cheaper to discard rather than repair it. This procedure, however, has not been followed as only one scaler has failed in three years, and this was due to the failure of the ceramic in a tubular condenser. This possibility has been eradicated by changing the component.

The High Voltage Flash Supply. The secondary current of a high voltage transformer was rectified by a 2X2 diode

and fed into a bank of 4-32 microfarad condensers which charged to 2500 volts. The 400 joules stored in these condensers was dissipated through the four flash lamps.

Illumination and Photography

Illumination was provided by four high-speed R 4340 Sylvania flash lamps which dissipated 100 joules each per flash. Each lamp was fitted with an aluminum foil reflector and a 2-1/2 x 6 inch cylindrical plastic collimating lens of 3-1/2 inch focal length, which was focused so that the image of the lamp was at the far side of the cloud chamber. The power supply for the flash lamps consisted of four 32 microfarad capacitors which were charged through a 2X2 high voltage diode. The ignition pulse was obtained from the secondary of an automobile ignition coil excited by the discharge of a thyratron through the primary. The resulting pulse had an extremely high voltage, but the overvoltage keeps the tubes active far beyond their normal life. The camera used was especially made for this task around an f4.5 Ektar lens. Approximately 450 pictures of the cloud chamber were obtained on each 100-foot roll of 35 mm film. It has been found that clear base Linagraph Ortho film is the most satisfactory for this use since it gives a good contrast at high film speed and has a fine grain.

IV CURVATURE MEASUREMENTS

The Standard Curves

The curvatures of the tracks were measured by comparison with standard curves which were prepared as follows: An arc of an ellipse which closely approximated a circular arc of the proper radius was inscribed in a heavy layer of Aquadag on a 4 x 7 glass plate by means of an Evans linkage. The glass plate was then moved .7 millimeter and a second curve of the same radius was inscribed. The result was a pair of parallel arcs separated by .7 millimeter. These arcs, of which there were several pairs per plate, were photographed using the same camera that was used to photograph the cloud chamber tracks and with the same distance between the camera and the plates as was used in the cloud chamber photography. The 35 mm negatives were projected through a machinist's comparator onto one half of a 5 x 7 Kodak 33 plate. Positive prints were made by contact printing on a second 5 x 7 Kodak 33 plate which was then cut lengthwise so that each group of standard curves was on a 2-1/2 x 7 glass plate. A strip of cellophane tape was put on the emulsion at each end so it would not be abraded by the ground glass of the comparator.

Comparison Methods

The machinist's comparator was fitted with a rotating 35 mm film holder and a proper illumination source for projection. The image was projected through an f4.5, 50 mm Ektar projection lens, similar to that used in the camera, onto the ground glass screen of the comparator. The actual measurement consisted of matching the projection of the track to the pair of curves having the same radius of curvature, whence the curvature of the original track was immediately known.

Although this method of measurement did not allow as precise a determination of the curvature of any single track as careful sagittal measurement, the method did permit fairly accurate measurements of the large number of tracks required in this study within a reasonable length of time.

V

DATA

The tracks to be measured were required to conform to the following criteria:

1. The track must be singly occurring except for tracks that are not coincident in time, such as old or post-expansion tracks.
2. The track must be counter controlled. The very few single tracks which passed through the chamber at such an angle that they apparently did not trigger both counters were considered to be a part of a shower.
3. The track must be at least 15 centimeters long.

The implications of the first criterion are manifold. First, it discriminates against dense showers and, in fact, against the electronic component in general. The 2.5 centimeters of lead above the chamber give a high probability for the multiplication of the electronic component. From the data of 1948 it is apparent that nearly all of the electronic component is eliminated in this manner. In addition, the single track criterion strongly discriminates against stars formed in the material directly above the chamber, but does

not strongly discriminate against stars formed some distance above the chamber due to the spreading of the particles.

Both of these results are desirable, since the characteristics of the undisturbed radiation were desired. The second criterion affects only a few tracks and tends to further discriminate against the electronic component. The third criterion should not affect any component preferentially.

The curvature of the tracks was measured by comparison with standard curves as noted before. There were twenty-four standard radii which fell on an exponential curve connecting 0.316 meter and 10 meters. These radii are given in Table I. The tracks were classified as being: equal to one of the standard curves, between two curves, greater than 10 meters (abbreviated by calling it infinite radius) or less than 0.316 meter. Thus, there were forty-nine radius intervals into which the tracks were classified. During the measurements the standard curves were designated by letters as a means of convenience.

The number of tracks falling into each class represents the momentum distribution of the cosmic rays which stop in the range interval for which the experiment was set up.

Since $P = 300 H\rho$ and $H = 5100$ for these experiments, it follows that $P = 0.25\rho$ within 2 per cent, if P is

expressed in Bev/C.

Due to the fact that the curvature measurements are somewhat uncertain and due to the statistical nature of the study, it is advisable to group several of the original forty-nine divisions together in order to obtain better definition of the individual points. In this manner Tables II to VI were constructed. As an alternate method of expression, these data are plotted in Figs. 8 to 12, where the rate is computed from the formula

$$R = \frac{C \cdot n \cdot T}{M \cdot F \cdot L}$$

R is the rate in particles per Bev/C per ster. per cm^2 per hr

L is the total number of tracks measured

C is the coincidence rate in particles per hour

n is the number of measured tracks in the momentum interval

M is the momentum interval

F is the total number of frames

TABLE I
RADII OF STANDARD CURVES

Letter	Rad. Curv. (meters)	Letter	Rad. Curv. (meters)
A	0.316	M	1.74
B	0.400	N	1.94
C	0.515	O	2.16
D	0.583	P	2.42
E	0.661	Q	2.73
F	0.751	R	3.08
G	0.852	S	3.51
H	0.966	T	4.06
I	1.09	U	4.81
J	1.23	V	5.85
K	1.39	W	7.41
L	1.56	X	10.00

TABLE II

MOMENTUM SPECTRUM
CASE AElev. 3.4 km - Climax
Oct - Nov 1949Moderating Lead 0 cm
Differential Lead 5 cm

Tracks

Positives	400	Average yield	36.7%
Negatives	157	C-A rate per hour	13.0 ± 0.2
Infinite - no sign	44	Single track rate	
Total measured	601	Conversion factor	0.0318
Total frames		Run	1,2,5,6,9,10

	No. of Particles		Radius of Curvature meters	+ Rate Particles hr ⁻¹ cm ⁻² (Bev/C) ⁻¹		- Rate ster ⁻¹		Momentum Bev/C
	+	-						
O-A	3.5	9	0.2	0.4	± 0.2	0.9	± 0.3	.05
A-C	12	22.5	0.42	1.9	± 0.5	3.6	± 0.8	.105
C-F	38.5	44	0.63	5.1	± 0.8	5.8	± 0.9	.151
F-H	16.5	24	0.86	2.5	± 0.6	3.5	± 0.7	.215
H-J	16.0	12	1.10	2.0	± 0.5	1.5	± 0.4	.275
J-L	15.0	11	1.40	1.4	± 0.3	1.1	± 0.3	.350
L-N	34.5	4	1.75	2.9	± 0.5	0.33	± 0.15	.488
N-O	77.5	5.5	2.18	5.1	± 0.5	0.36	± 0.2	.545
P-R	65.5	3	2.75	3.2	± 0.4	0.15	± 0.08	.688
R-T	46.5	4	3.57	1.5	± 0.2	0.13	± 0.06	.892
T-V	37.0	1.5	4.96	0.66	± 0.1	0.02		1.24
V-X	24.5	5.5	7.93	0.19	± 0.04	0.04		1.90

TABLE III

MOMENTUM SPECTRUM
CASE BElev. 3.4 km - Climax
Oct - Nov 1949Moderating Lead 5 cm
Differential Lead 10 cm

Tracks

Positives	482	Average yield	58.9%
Negatives	231	C-A rate per hour	13.6
Infinite - no sign	20	Single track rate	
Total Measured	733	Conversion factor	0.044
Total frames	1812	Runs	10,11,12,13,14

	No. of Particles		Radius of Curvature	+ Rate	- Rate	Momentum
	+	-		Particles hr ⁻¹ cm ⁻² (Bev/C) ⁻¹	ster ⁻¹	Bev/C
O-A	0	0	0.2	0	0	.05
A-C	0	1.5	0.42	0	0.3 ± 0.2	.105
C-F	4.5	0.5	0.63	0.8 ± 0.3	0.1	.151
F-H	35	11.5	0.86	7.0 ± 1.0	2.3 ± 0.7	.215
H-J	63	58	1.10	10.7 ± 1.3	9.7 ± 1.3	.275
J-L	71.5	58.5	1.40	9.5 ± 1.1	7.8 ± 1.0	.350
L-N	34.5	36	1.75	4.0 ± 0.7	4.2 ± 0.7	.488
N-P	26.5	22.5	2.18	2.4 ± 0.5	2.1 ± 0.4	.545
P-R	57.5	16	2.75	3.8 ± 0.5	1.1 ± 0.3	.688
R-T	77.5	9.5	3.57	3.5 ± 0.4	0.4 ± 0.1	.892
T-V	50.5	7	4.96	1.2 ± 0.1	0.2 ± 0.1	1.24
V-X	41.5	4.5	7.93	0.5 ± 0.1	0.1	1.98

TABLE IV

MOMENTUM SPECTRUM
CASE CElev. 3.4 km - Climax
November 1949Moderating Lead 15 cm
Differential Lead 10 cm

Tracks

Positives	414	Average yield	62.4%
Negatives	265	C-A rate per hour	9.2 ± 0.4
Infinite - no sign		Conversion factor	0.0307
Total measured		Runs	15, 16, 17, 18
Total frames	1744		

	No. of Particles		Radius of Curvature	+ Rate	- Rate	Momentum
	+	-	meters	Particles hr ⁻¹ cm ⁻² (Bev/C) ⁻¹	ster ⁻¹	Bev/C
O-A	3	0	0.2	0.2	0	.05
A-C	0	0	0.42	0	0	.105
C-F	0	1	0.63	0	0	.151
F-H	0	0	0.86	0	0	.215
H-J	1	1.5	1.10	0.1	0.2	.275
J-L	31	18.5	1.40	2.9	1.7	.350
L-N	76.5	63.5	1.75	6.2	5.1	.488
N-P	50.5	64.5	2.18	3.2	4.1	.545
P-R	53	41	2.75	2.5	1.9	.688
R-T	48	29.5	3.57	1.5	0.9	.892
T-V	78	19	4.96	1.3	0.3	1.24
V-X	73	26	7.93	0.5	0.2	1.98

TABLE V

MOMENTUM SPECTRUM
CASE DSea Level - Seattle
April, May 1950Moderating Lead None
Differential Lead 5 cm

Tracks

Positives	383	C-A rate per hour	$2.3 \pm .05$
Negatives	235	Single track rate	1.02
Infinite - no sign	22	Conversion factor	0.0064
Total measured	640	Runs	S-1,2,3,4,5,6,7
Total frames			

	No. of Particles		Radius of Curvature	+ Rate		- Rate		Momentum
				Particles hr ⁻¹				
	+	-	meters	cm ⁻²	(Bev/C) ⁻¹	ster ⁻¹		Bev/C
O-A	12.5	12	0.2	0.3	± .08	0.3	± .08	.05
A-C	26.0	37	0.416	0.9	± .16	1.2	± .2	.104
C-F	72.5	70.5	0.633	2.0	± .2	1.9	± .2	.158
F-H	53.0	44.5	0.859	1.6	± .2	1.3	± .2	.215
H-J	13.0	11.5	1.10	0.5	± .16	0.4	± .1	.275
J-M	24.0	9.5	1.49	0.3	± .06	0.12	± .04	.373
M-P	32.0	13.0	2.08	0.3	± .05	0.12	± .03	.520
P-S	37.0	6.5	2.97	0.22	± .04	0.04	± .015	.743
S-U	25.5	3.5	4.16	0.13	± .02	0.02	± .01	1.04
U-W	29.5	8.5	6.11	0.07	± .01	0.02	± .007	1.53
W-X	22.0	7.5	8.7	0.05	± .01	0.02	± .006	2.18

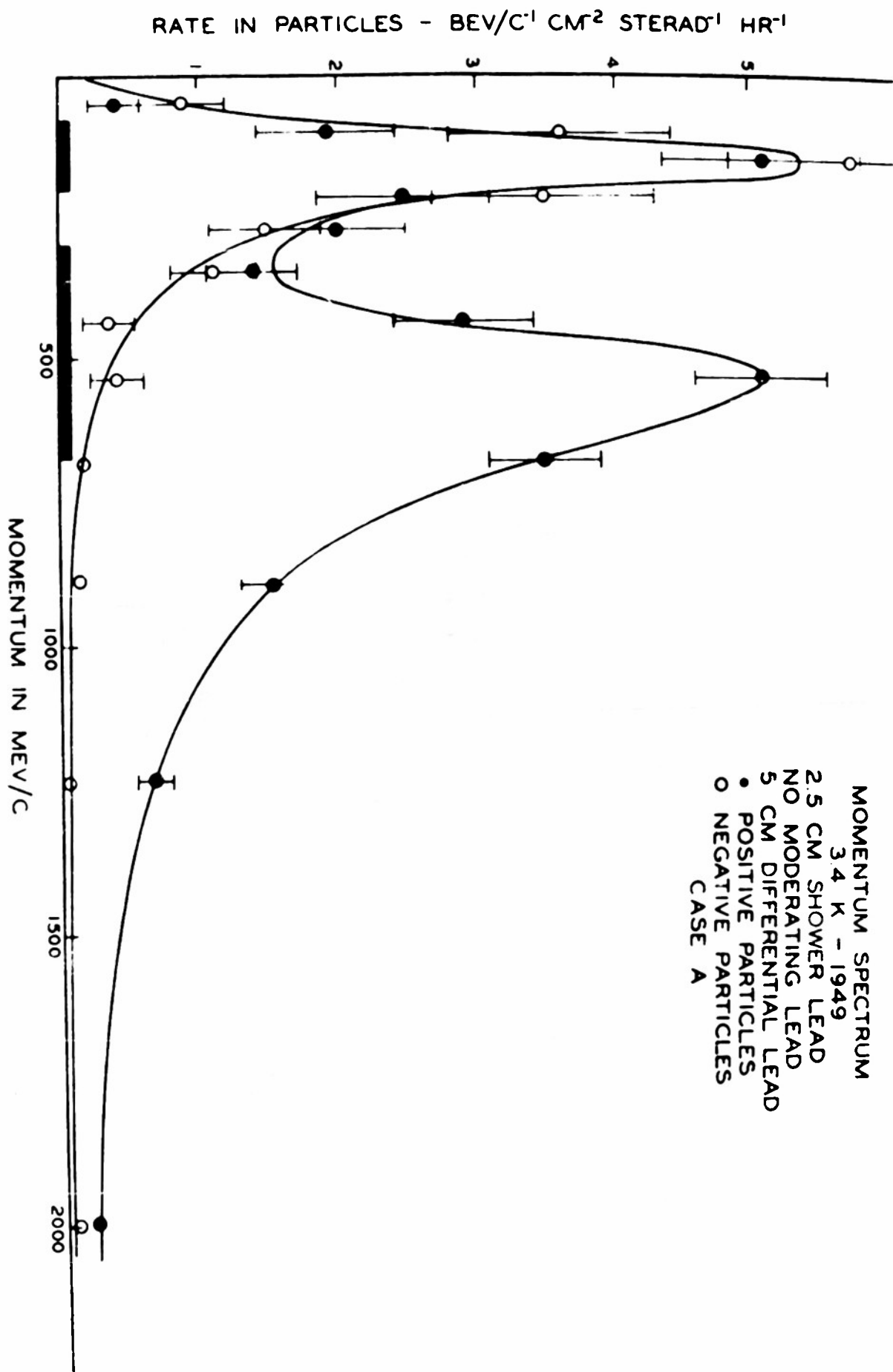
TABLE VI

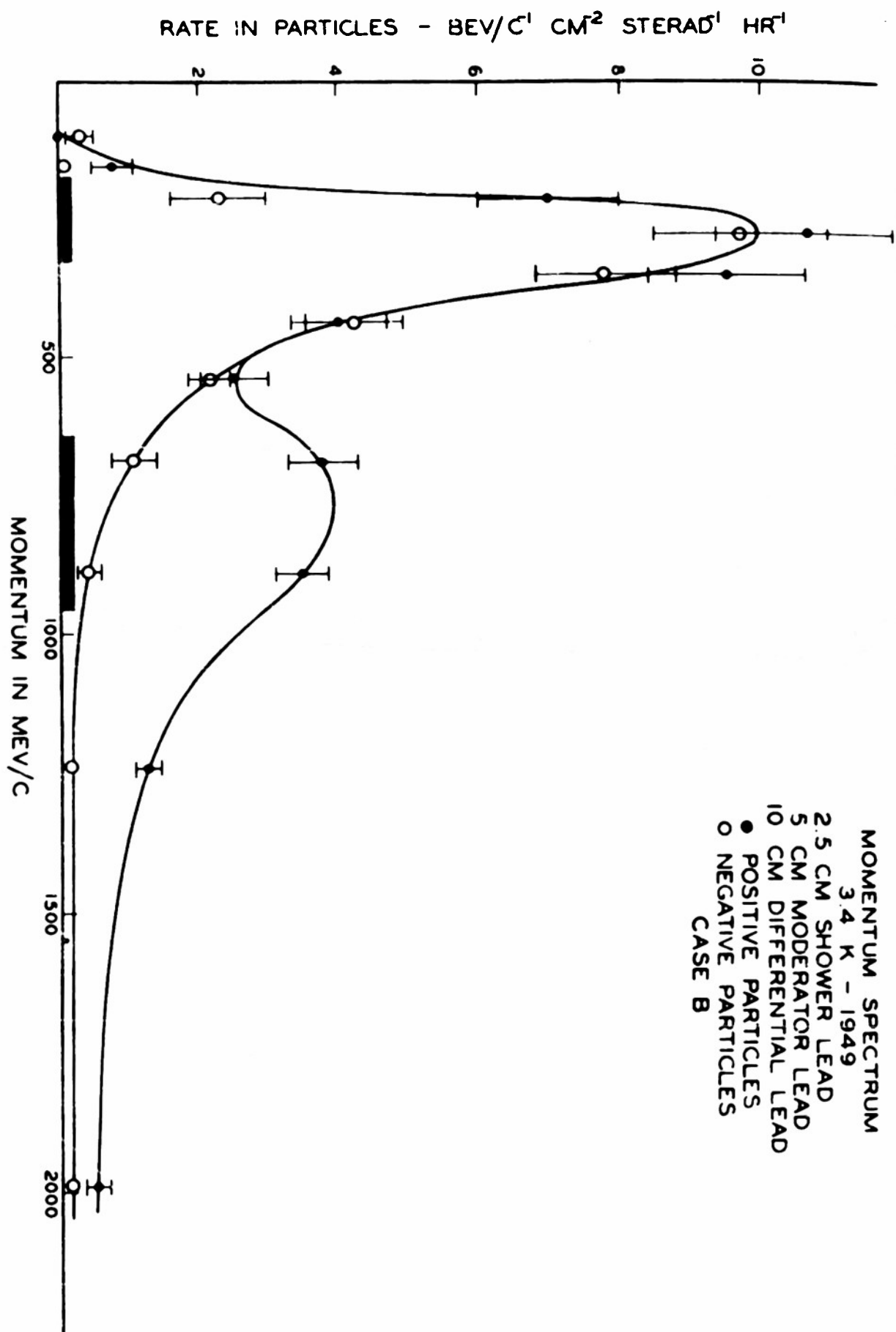
MOMENTUM SPECTRUM
CASE ESea Level - Seattle
June 1950Moderating Lead None
Differential Lead 10 cm

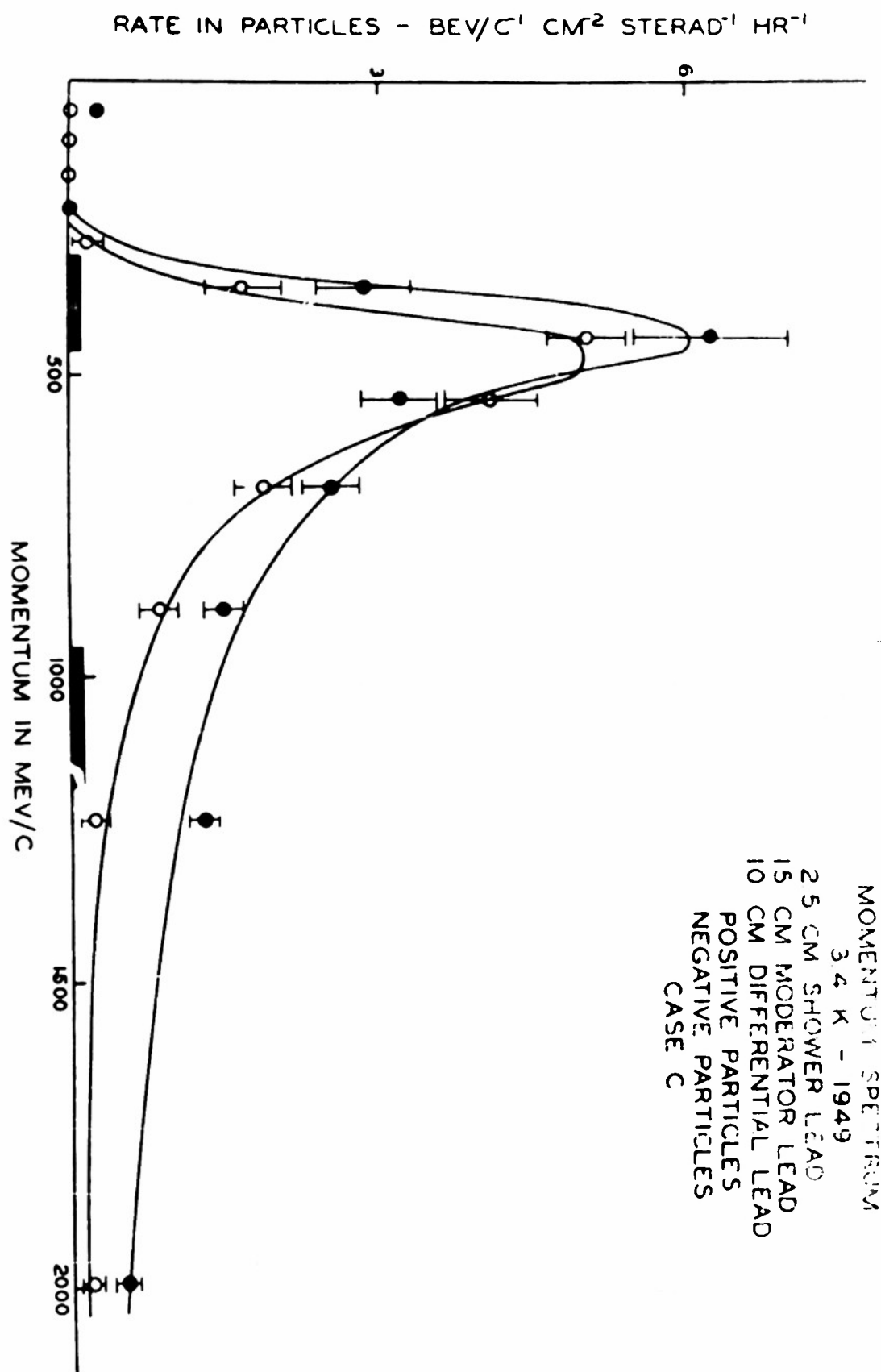
Tracks

Positives	454	C-A rate per hour	$3.48 \pm .14$
Negatives	318	Single track rate	$1.76 \pm .09$
Infinite - no sign	12	Conversion factor	0.0090
Total measured	784	Runs	B-1,2,3,4,5,6
Total frames	2250		

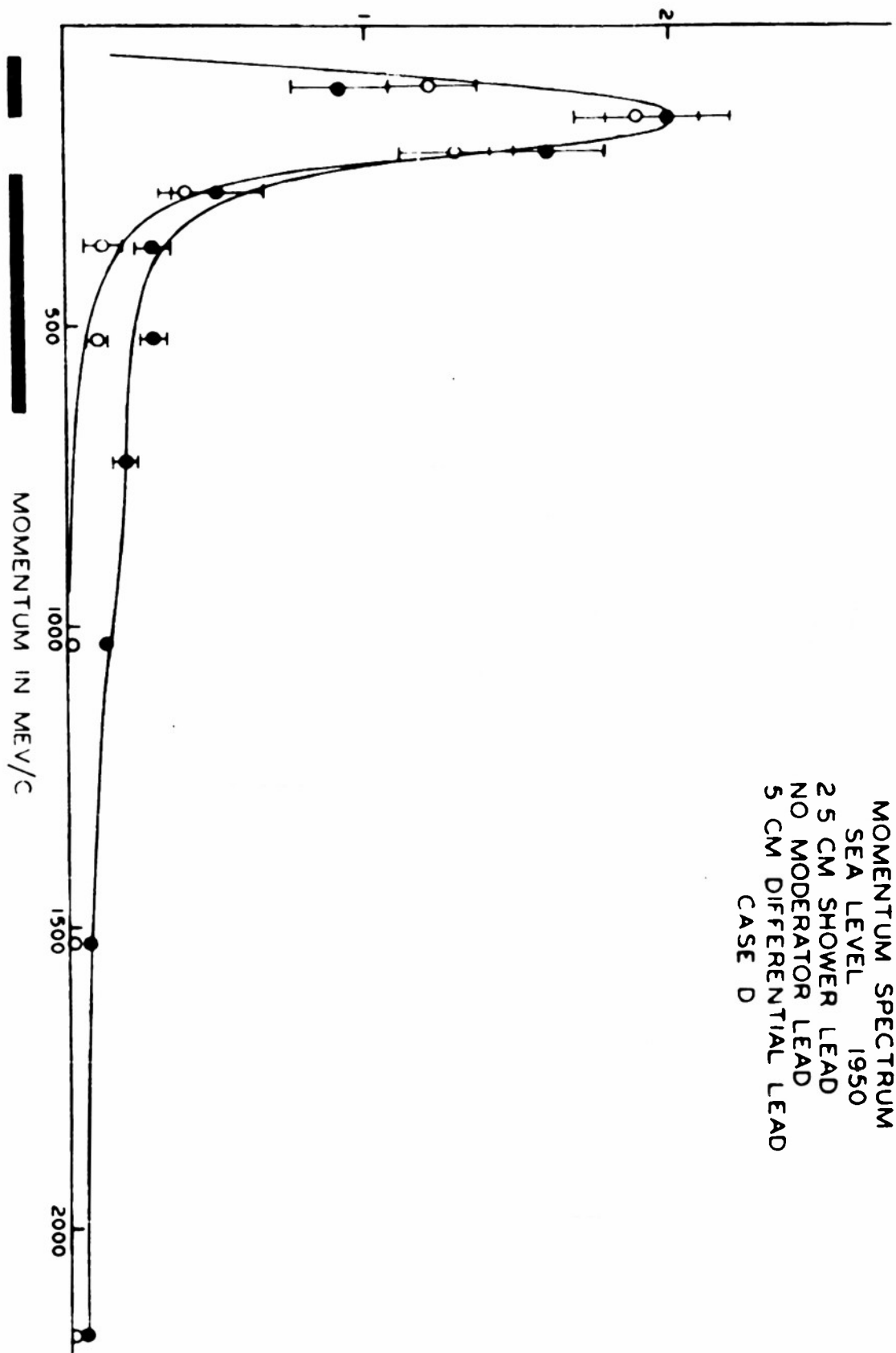
	No. of Particles		Radius of Curvature meters	+ Rate		- Rate	Momentum
	+	-		Particles hr ⁻¹ cm ⁻² (Bev/C) ⁻¹		ster ⁻¹	Bev/C
O-A	12	12.5	0.2	$0.34 \pm .1$		$0.36 \pm .1$.05
A-C	25.5	32	0.416	$1.15 \pm .23$		$1.45 \pm .26$.104
C-F	58.5	65	0.633	$2.23 \pm .29$		$2.48 \pm .31$.158
F-H	74.5	88.5	0.86	$3.12 \pm .37$		$3.70 \pm .40$.215
H-J	79.5	69	1.10	$2.71 \pm .31$		$2.35 \pm .28$.275
J-M	28.5	17.5	1.49	$0.50 \pm .09$		$0.31 \pm .07$.373
M-P	25	11	2.08	$0.33 \pm .07$		$0.15 \pm .05$.520
P-S	47	6	2.97	$0.39 \pm .06$		0.05	.743
S-U	41	2.5	4.16	$0.28 \pm .04$		0.02	1.04
U-W	25	2	6.11	$0.09 \pm .02$		0.01	1.53
W-X	12	1.5	8.7	$0.04 \pm .015$		0.01	2.18





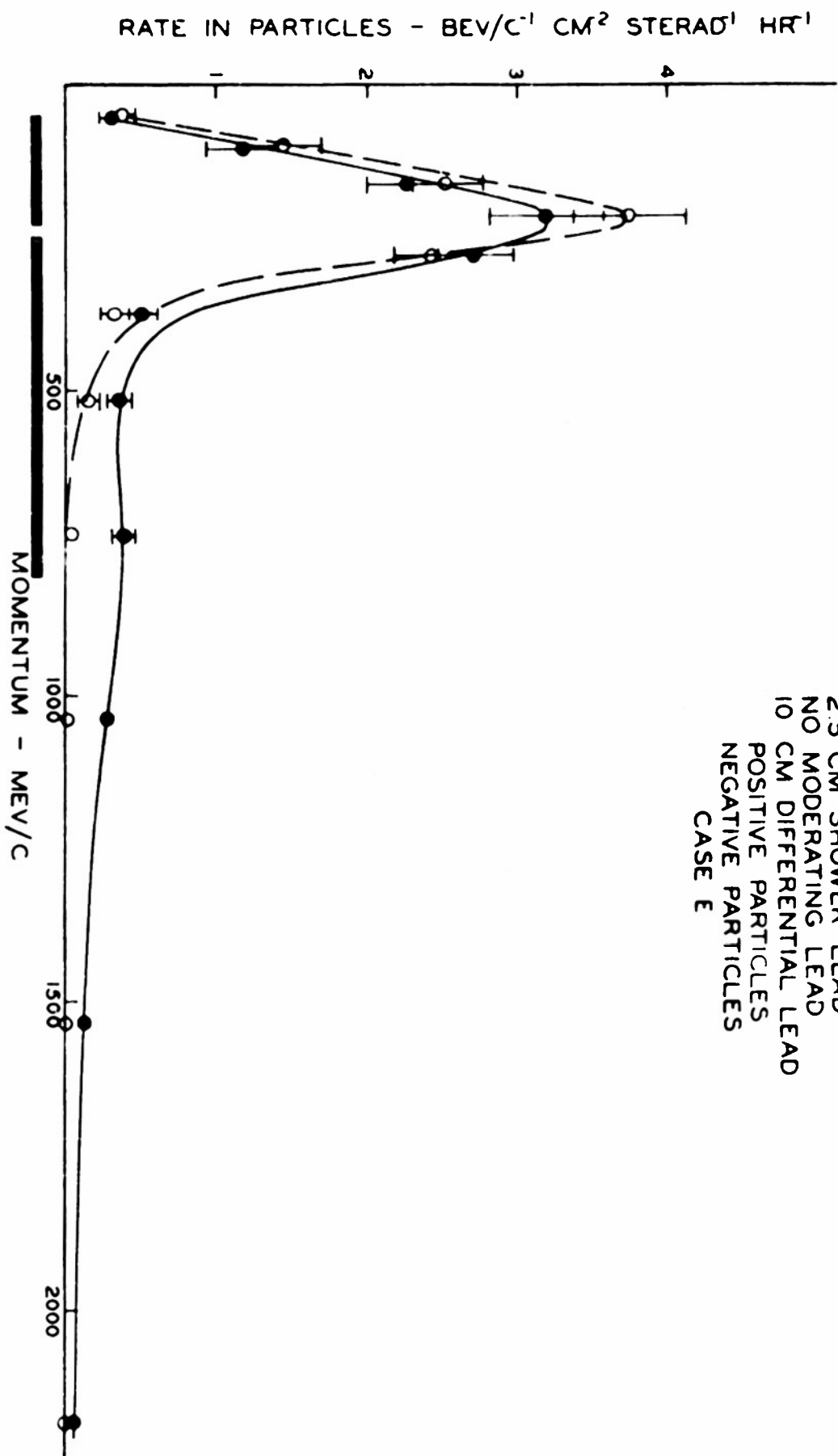


RATE IN PARTICLES - BEV/C⁻¹ CM² STERAD⁻¹ HR⁻¹



MOMENTUM SPECTRUM
SEA LEVEL 1950
2.5 CM SHOWER LEAD
NO MODERATOR LEAD
5 CM DIFFERENTIAL LEAD
CASE D

MOMENTUM SPECTRUM
 SEA LEVEL 1950
 2.5 CM SHOWER LEAD
 NO MODERATING LEAD
 10 CM DIFFERENTIAL LEAD
 POSITIVE PARTICLES
 NEGATIVE PARTICLES
 CASE E



VI

ERRORS AND CRITICISMS

The most cogent criticisms of this work are, first, the inclusion of counter C, and, second, the design of the anti-coincidence tray D. Any advantage obtained by the third coincidence tube in the elimination of showers is overshadowed by scattering losses of mesons and by scattering and nuclear losses of protons. Secondly, the anticoincidence coverage in tray D was borderline. Although it sufficed for the five centimeter case, the results of other cases are somewhat more doubtful. It was clearly realized after the 3.4 kilometer data were plotted that any attempt to measure the sea level proton flux would certainly meet with little success unless the anticoincidence tray was redesigned completely. Some fourteen tubes were included in the new model (shown in Fig. 13) which gave far more complete coverage than the one used at 3.4 kilometers. Due to the large area covered by the tubes, 1N34 germanium crystal diodes were put in the input of each Geiger tube in order to isolate the tube from the rest of the tray. This resulted in a minimum leakage of particles due to dead time of the tubes. The cutoff is seen to be far better than with the previous anticoincidence tray. The advantages derived from the elimination of tray C was so great

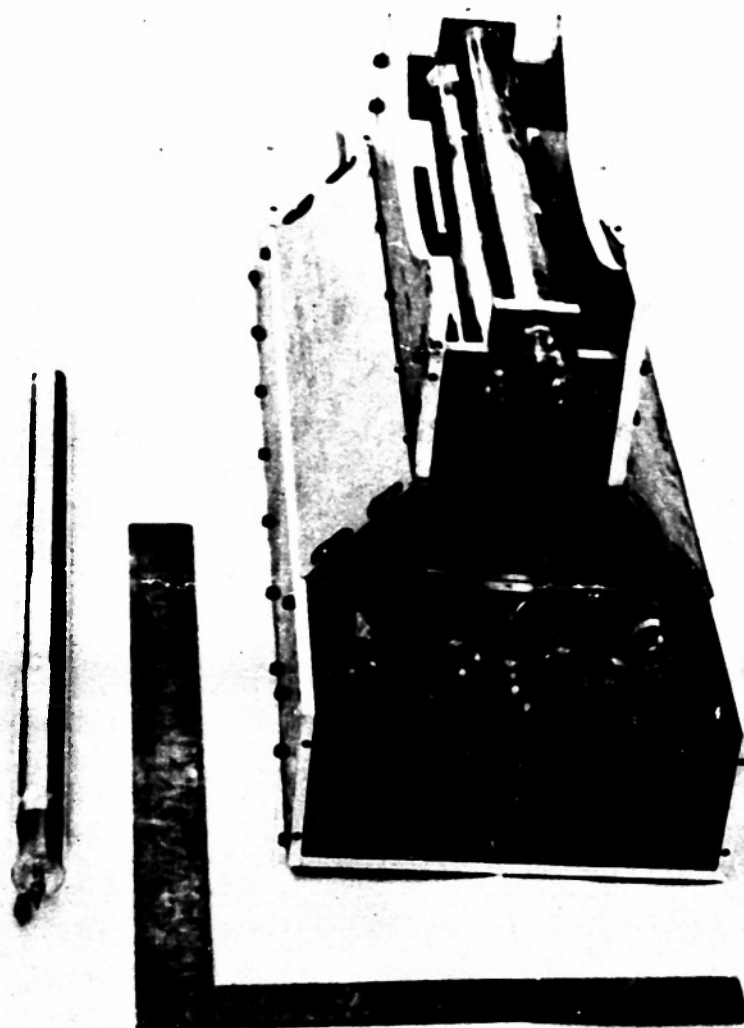


FIGURE 13. ANTICOINCIDENCE TRAY

that the way is clearly pointed towards a new experiment which has as a basic philosophy the separation of protons from mesons by their nuclear reaction, a process that has been utilized here as a secondary method for which the experiment was not designed. This approach forms the basis of a succeeding experiment which is not a part of this experiment.

The question of the electronic component will be considered before scattering corrections. The total single track spectrum and the single track spectrum under various layers of lead were found in 1948 using the same cloud chamber and a counter telescope consisting of counters A and B (references 34,37). It was found that the high peak due to electrons was entirely gone when the spectrum of singly occurring tracks was measured under 5 centimeters of lead. Further increases in the lead absorber above the cloud chamber did not change the shape of the spectrum appreciably. The layer of lead above the chamber was decreased to 2.5 centimeters for the present study. Comparison of the meson peak of Fig. 1 with the meson spectrum found in the previous work (given in Fig. 4) shows that few, if any, electrons are included in the present work. Further evidence is obtained from the negative meson intensity at higher momenta. Positrons and negatrons would have about the same behavior in passing through matter. In any event, the flux of positrons should not be greater than negatrons

at high momenta, but the spectrum of negative particles shows that this intensity must be small.

The proton intensity among those particles stopped in 0.5 to 5.5 centimeters of lead in an ideal experiment should be the intensity of the positive curve above the meson cutoff. An error of inclusion occurs when a particle passes through counters A, B, and C and scatters in the differential lead in such a manner that it fails to trigger one of the anticoincidence counters D. This effect is small (its magnitude is measured by the magnitude of the negative curve at high momenta). The correction for this effect is to subtract the negative curve from the positive curve. This assumes that the positive excess is one, an assumption that does not have to be rigorously correct, since the residual negative curve is so small compared to the positive curve that a positive excess of 1.5 or more would not change the measured proton flux appreciably.

Errors of exclusion occur when a particle passes through counters A and B and scatters in the moderating absorber in such a manner that it fails to reach counters C. The computation of this effect will now be carried out.

An approximation method, based on the diffusion equation given by Rossi and Greisen (5) will be used. The assumption made is that if a particle is displaced laterally to the edge of the counter it can be considered lost. This

is not a true picture, since the particles at this point will travel in all directions, but this effect is compensated by those particles which are not displaced this far but travel in such direction as to miss counters C.

Equation 1.64 of Rossi and Greisen is

$$H(t, y) = \int_{-\infty}^{\infty} F(t, y, \theta) d\theta = \frac{\sqrt{3}}{2\sqrt{\pi}} \frac{W}{t^{3/2}} e^{-\left[\frac{3}{4} \frac{W^2 y^2}{t^3}\right]}$$

$$W = \frac{2 P \beta}{E_s}$$

where E_s = a characteristic energy with a numerical value of 21 Mev

t = the depth of the absorber, measured in terms of radiation lengths equal to 5.9 gm/cm²

y = lateral displacement in cm

The computation will be carried through for case C first, since it is the only one that has significant scattering corrections. The lateral displacement required to miss counter C is approximately 3.18 cm, hence the particles lost are given by

$$S = 2 \int_{3.18}^{\infty} H(t, y) dy = 2 \int_{3.18}^{\infty} \left[\frac{\sqrt{3}}{2\sqrt{\pi}} \frac{W}{t^{3/2}} e^{-\left[\frac{3}{4} \frac{W^2 y^2}{t^3}\right]} \right] dy$$

A change of variables simplifies the problem.

Set

$$\frac{3W^2y^2}{4t^3} = \frac{\phi^2}{2}$$

then $S = \int_{\frac{3.18\sqrt{\frac{3}{2}} \frac{W}{t^{3/2}}}}^{\infty} \left[e^{-\frac{\phi^2}{2}} \right] d\phi$

For case C

$$\frac{1}{X_0} = 4\alpha \frac{N}{A} Z^2 r_0^2 \log(183)^{-\frac{1}{3}}$$

$$X_0 = 5.9 \text{ centimeters of lead}$$

$$t = \frac{15.5 \times 11.5}{5.9} = 30.2 \text{ radiation lengths}$$

The value of W is found first for the meson peak for which

$$p = 450 \text{ Mev}/c$$

$$E = 400 \text{ Mev}/c$$

Then

$$\beta = \frac{pc}{E + mc^2} = .97$$

$$W = \frac{2\beta p}{21} = 41.6$$

Numerical evaluation of the lower limit of integration gives

$$\phi_1 = 3.18 \sqrt{\frac{3}{2}} \frac{W}{t^{3/2}} = 3.18 \times 1.22 \times \frac{41.6}{166} = 0.875$$

Then $S = \int_{0.875}^{\infty} e^{-\frac{\phi^2}{2}} d\phi$

This integral is the Gaussian distribution integral and is evaluated in many tables (40). From the tables $S = 0.4$.

If this correction is applied to the negative meson peak, it is found to coincide with the momentum spectrum found in 1948 by Miller, Henderson, et al.

A similar correction must also be computed for protons. The detail will not be given here, since it is similar to the above computation. The correction factors derived from such computations are tabulated below:

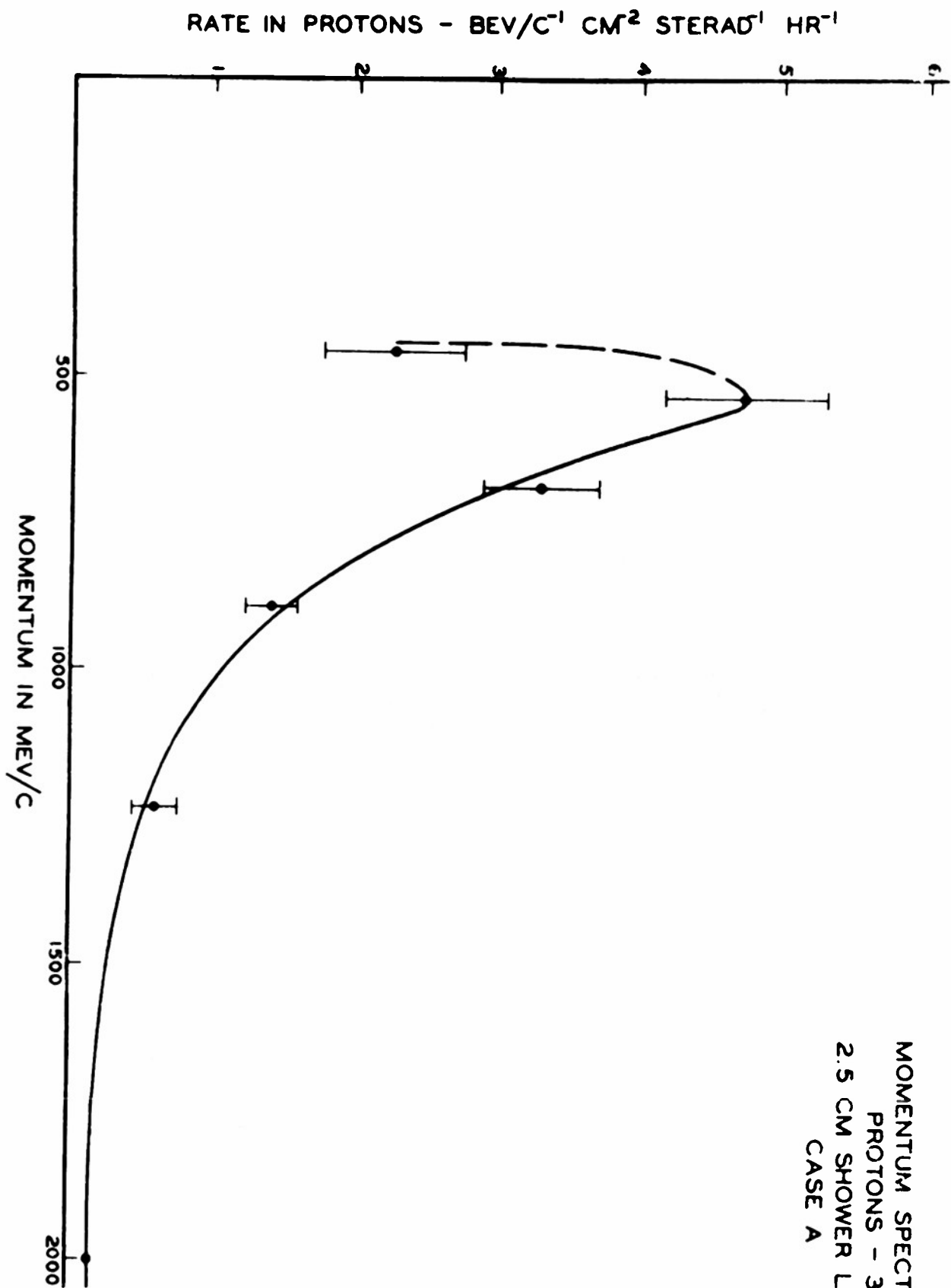
Case	Mesons	Protons
A	1.00	1.00
B	1.01	1.00 { 750 Mev/C }
C	1.66	1.28 { 800 Mev/C }
		1.16 { 1 Bev/C }
		1.06 { 1.25 Bev/C }

Thus it is seen that this particular scattering correction is necessary only in case C.

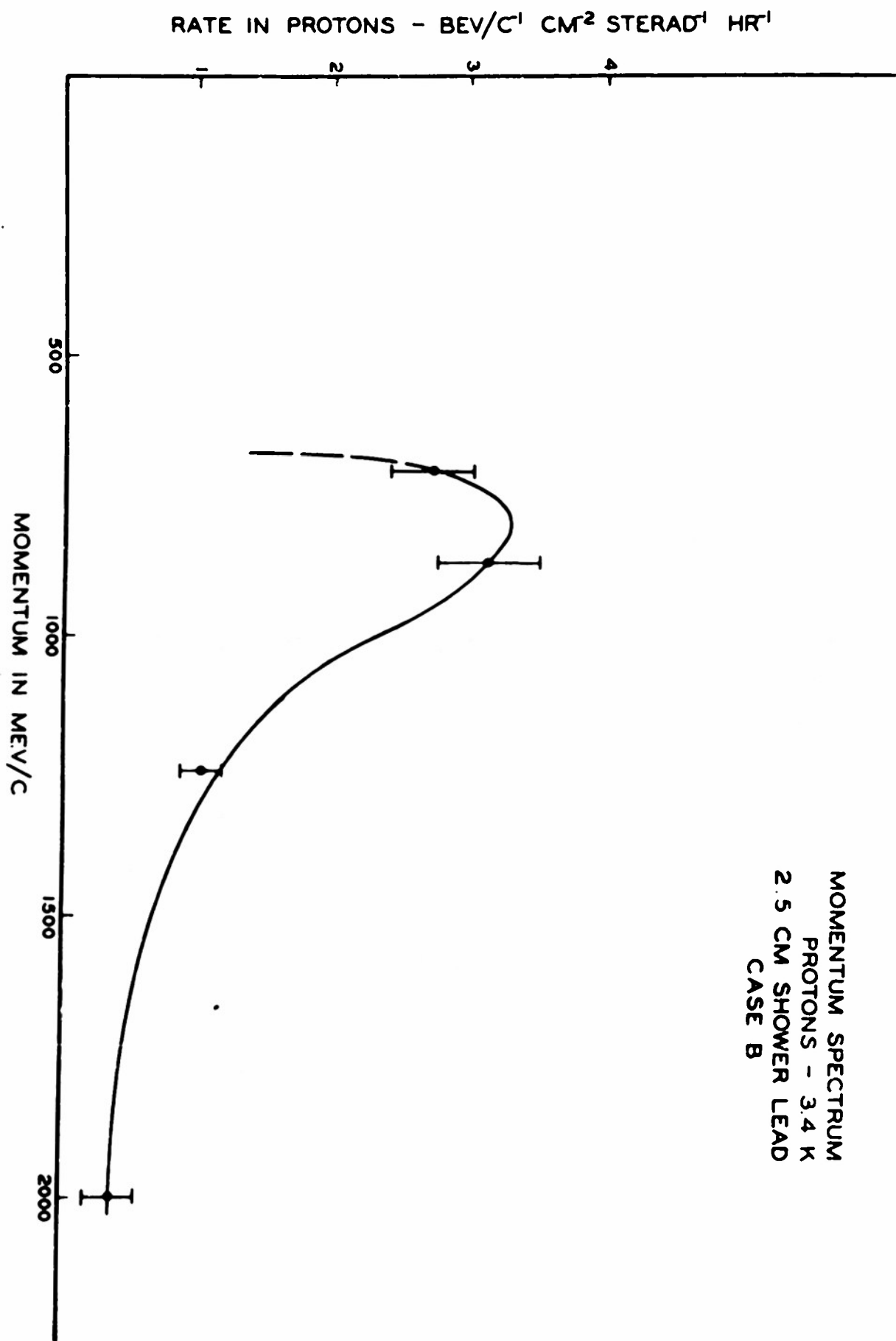
The right hand side of the second peak does not fall off as rapidly as would be expected because of small angle scattering. It was noted in the experimental method that it could be expected that some very high momentum protons would be stopped in the differential lead. As the differential lead is increased, the number of protons penetrating the absorber is in agreement with an exponential absorption law, thus verifying the hypothesis that protons absorbed by

catastrophic collisions are the cause of the high counting rate above 1 Bev/C. The proton intensities found in the three cases are plotted in Figs. 14 to 16.

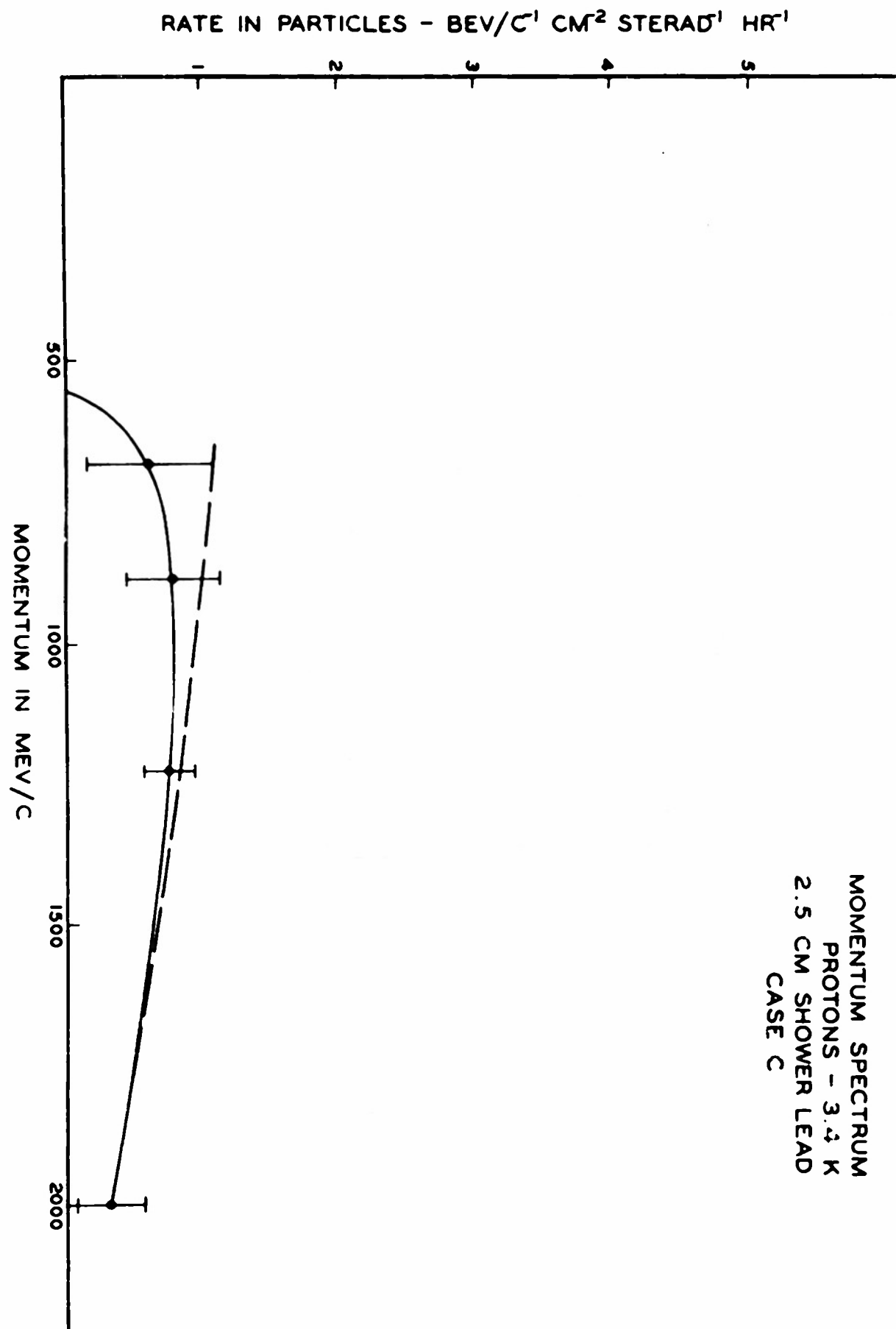
There is one more correction to the proton spectrum which will be evaluated, but which is not included in the curves, which give the proton spectra in the chamber itself. Those protons absorbed in the material up to counter C will not be recorded. This absorber is equivalent to about three and one-half centimeters of lead or about a quarter of a mean free path. The intensity in the atmosphere should then be about 1.28 times the intensity reported here.



MOMENTUM SPECTRUM
PROTONS - 3.4 K
2.5 CM SHOWER LEAD
CASE A



MOMENTUM SPECTRUM
PROTONS - 3.4 K
2.5 CM SHOWER LEAD
CASE B



VII RESULTS

Discussion of Momentum Distribution Found

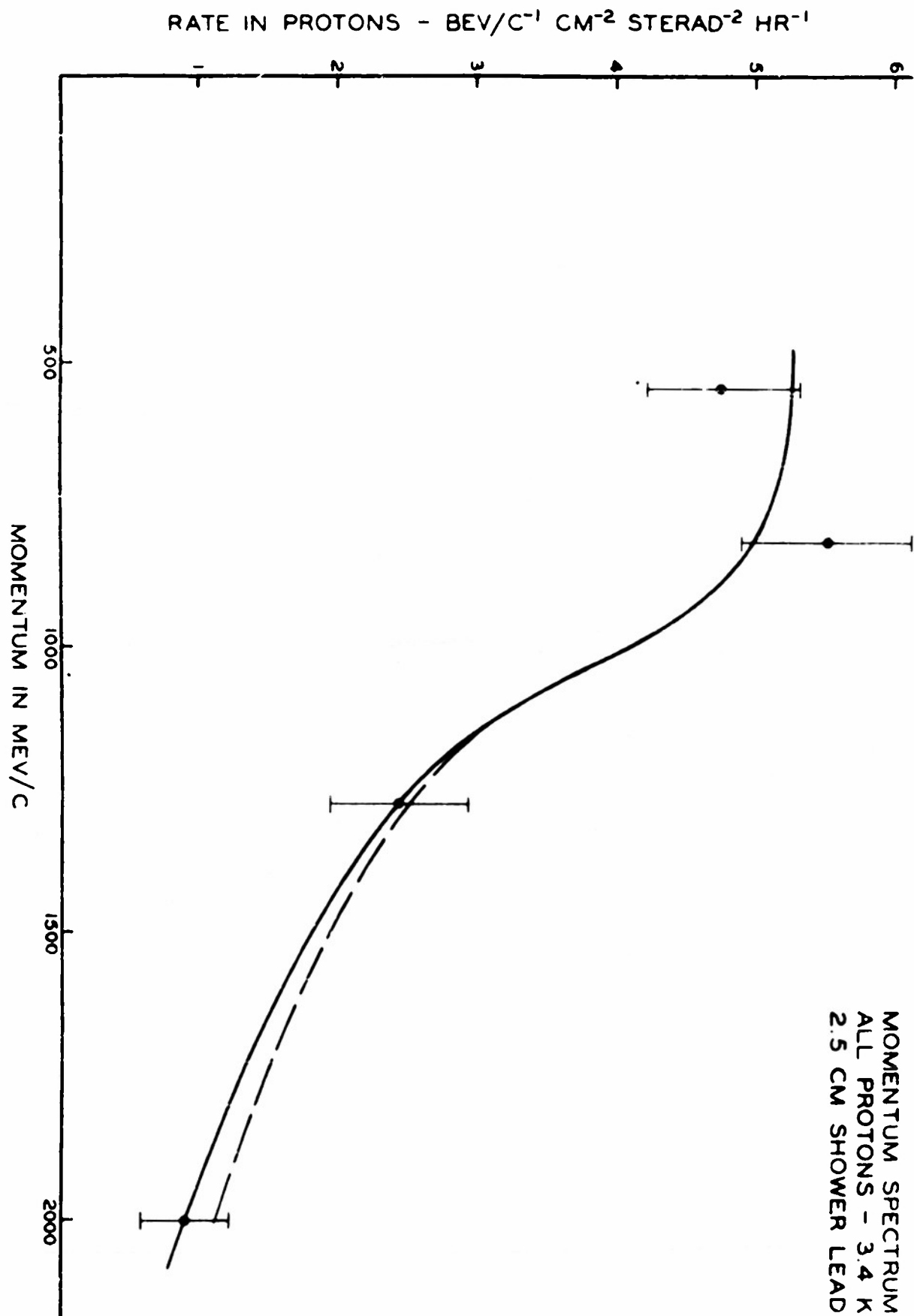
The momentum distribution of those particles which have ranges between 0.5 and 5.5 centimeters of lead (Fig. 9) shows two peaks for positive particles and only one peak for negatives. If the left slope of the second peak is continued to intersect with the axis, it is found that the zero of the extrapolated curve is at 300 Mev/C, which is just the momentum a proton would have to have to penetrate from the sensitive volume of the cloud chamber to the sensitive volume of counter C. Beyond the second peak the positive intensity is always measurably higher than the negative intensity. A meson having a momentum greater than 200 Mev/C should penetrate the 5.5 centimeters of lead, trigger the anticoincidence counter, and thus not be photographed. It is true that, although the slope on the right side of the peak is very steep, it is still far from vertical. This finite slope is largely due to scattering in the 5 centimeter layer of lead and also due to some leakage through and around the anticoincidence tray D. The effect of scattering has already been discussed.

The following two facts indicate clearly that the particles causing this peak are actually protons. First, the second peak occurs only in the positive spectrum, and second, the low momentum cutoff is at the momentum that a proton would require to get from the sensitive volume of the cloud chamber to the sensitive region of tray C. Ionization density checks show that many of these particles are heavily ionizing but that not all protons, even of relatively low momenta, could have been picked out in this manner.

The Proton Spectrum

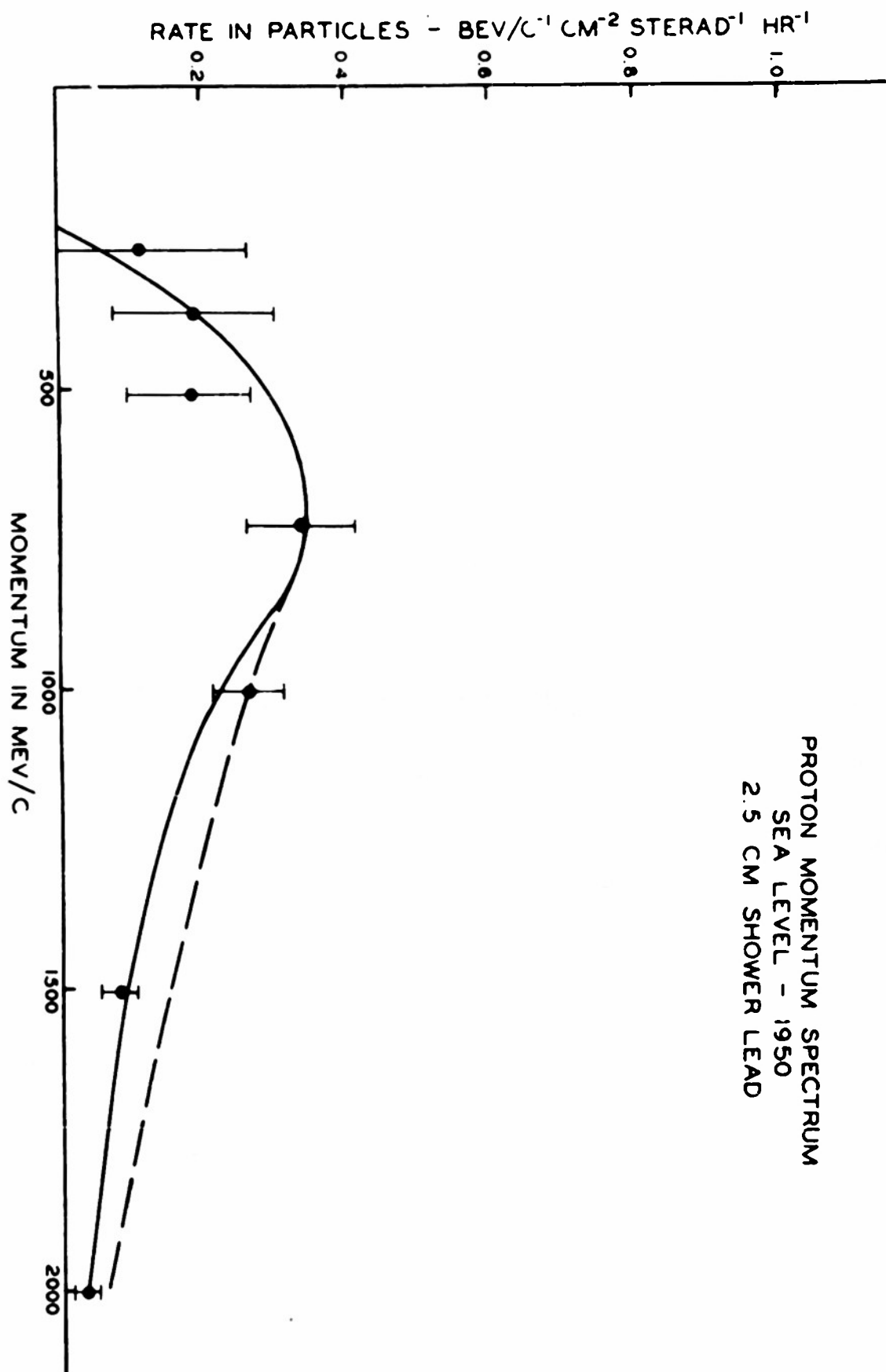
The proton spectrum found at 3.4 kilometers is shown in Fig. 17. This was obtained by adding the spectra found in cases A, B, and C. It is this addition which adds to the statistical errors of the final estimate. An experiment designed to make use of nuclear interactions rather than ionization absorption would avoid this addition and hence would reduce the statistical uncertainties. A correction for the protons which are not absorbed by nuclear interaction as they pass through the lead has been made at momenta above 1.25 Bev/c.

The proton spectrum at sea level (Fig. 18) has been computed for those protons absorbed in 10 centimeters of lead. Only about 60 per cent of the number of protons above



MOMENTUM SPECTRUM
ALL PROTONS - 3.4 K
2.5 CM SHOWER LEAD

PROTON MOMENTUM SPECTRUM
SEA LEVEL - 1950
2.5 CM SHOWER LEAD

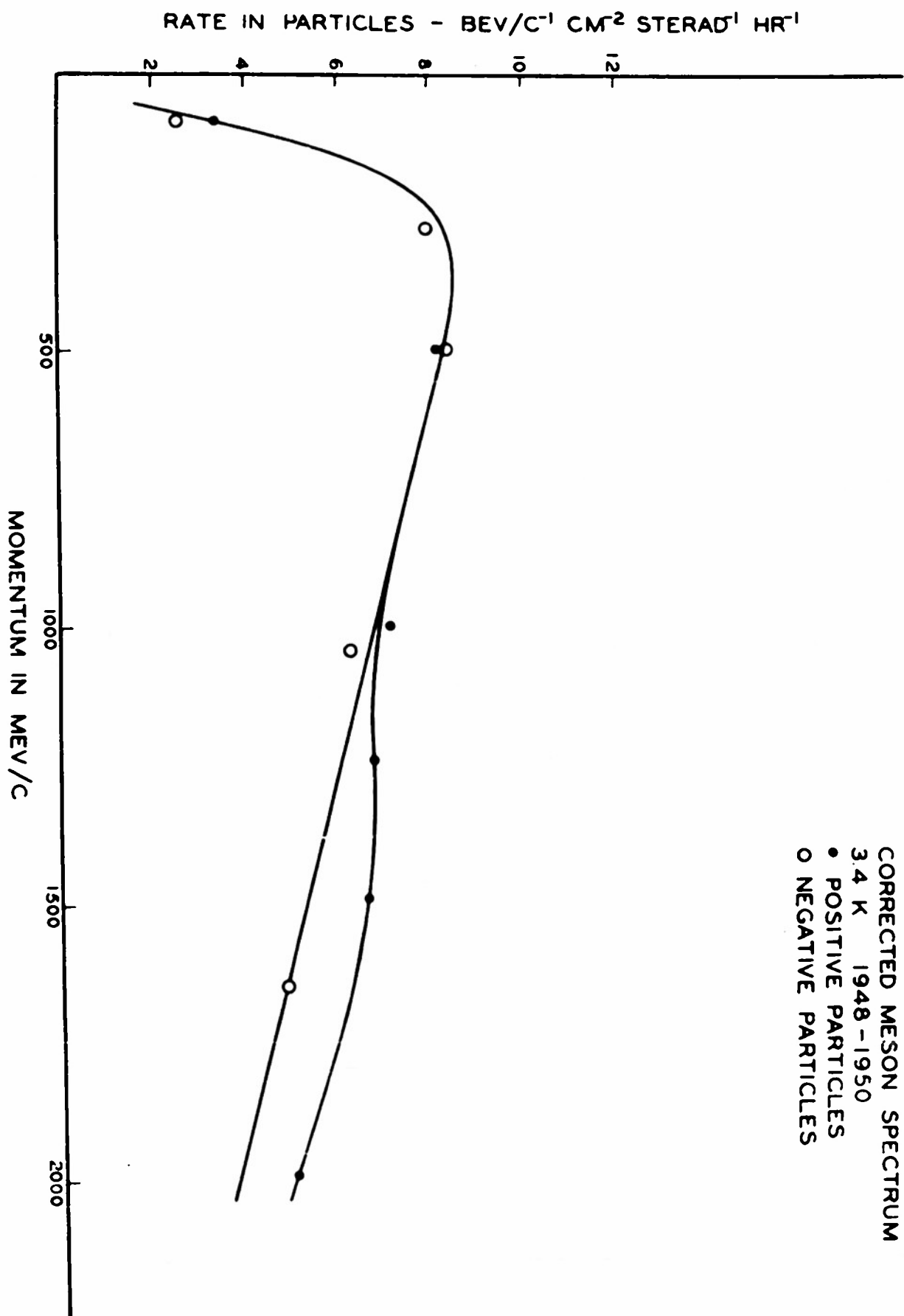


750 Mev/C are absorbed in the lead.

The various corrections mentioned in the appropriate sections have all been made in these curves.

The Meson Spectrum

If the proton momentum spectrum is subtracted from the momentum spectrum of positive particles under 5 centimeters of lead found by Miller, Henderson, et al, a second approximation to the true meson flux is obtained. The corrected meson spectrum is shown in Fig. 19. The positive and negative meson spectra then coincide up to a momentum of 1 Bev/C (and within statistics up to 1.25 Bev/C). After this momentum has been exceeded, there appears to be a real positive excess. One possible explanation of this is that if a proton and neutron interact in a simple exchange collision, the proton would still have a high probability of completely traversing the remaining lead. Another possibility is that mesons of sufficient energy to traverse the remaining lead are generated in the nuclear collisions. Examination of the energy equation indicates that such transitions are possible. That similar events occur in the upper atmosphere has been amply verified (see references 22, 23, 24). The net result of such processes would be that the path length for removal would be increased, which would lead



to too low an estimate of the proton flux. If such processes are the correct explanation of the positive excess shown above 1.25 Bev/C, then the cross-section for such events is approximately half the total cross-section for interaction of protons having a momentum of about 2 Bev/C with lead nuclei.

Mean Free Path in Lead

A mean free path for protons in lead can be computed from the results of the present investigation, but the probable error is nearly twice that quoted for the counter studies. The direct evaluation of this problem requires the solution of a fifth degree equation; however, an approximate calculation will give enough information to permit a second order approximation. The solution depends on the comparison of the number of protons stopping in 5 centimeters of lead with high enough momenta so that they would penetrate the lead if only ionization losses were important, compared to those stopping in 25 centimeters of lead. The results of case C will be corrected for scattering as noted in the previous discussion.

Taking those protons with momenta equal to or greater than 690 Mev/C (slightly higher than the ionization loss cutoff), the integrated proton flux in the three cases is as follows:

	Case A	Case B	Case C
Proton Flux (cm ⁻² sterad ⁻¹ hr ⁻¹)	5.11	8.27	4.32

The sum of all three is 15.14 protons (Bev/C)⁻¹ cm⁻² sterad⁻¹ hr⁻¹

Then

$$5.11 = 17.72 \times (1 - e^{-5/L})$$

$$L = 14.7 \text{ cm or } 169.5 \pm 30 \text{ gm/cm}^2$$

When the results are corrected for transmission of protons through the 25 centimeters of lead, the mean free path is $174 \pm 30 \text{ gm/cm}^2$. The results of case B permit a check on this figure. The mean free path computed from this case is in excellent agreement with 174 gm/cm^2 . The value is somewhat higher than the 160 gm/cm^2 usually quoted for the "N" component, but the statistical uncertainties are so great that the difference is not significant. This measurement is of sufficient importance that a direct study of the problem using an experiment designed for the direct study of nuclear absorption is desirable, as the probable error would be reduced by a factor of two or more, especially at higher momenta.

Mean Free Path of the "N" Component in the Atmosphere

The proton intensities found at 3.4 kilometers and at sea level provide enough data to permit the computation

of a mean free path for removal of the radiation which creates 0.75 to 2 Bev/C momentum protons. It shall be assumed in this thesis that the radiation responsible for the generation of protons in this momentum interval is the Rossi "N" component, and it shall be discussed from this standpoint.

If the proton momentum spectra are integrated from 0.75 Bev/C to 2 Bev/C at sea level and at 3.4 kilometers, the resulting fluxes can be compared directly. Partial justification for this procedure can be found in that the momentum spectra found at the two altitudes are approximately the same shape.

The integrated fluxes are as follows:

	Flux (Protons cm ⁻² sterad ⁻¹ hr ⁻¹)
Sea level	0.94 ± .09
3.4 kilometers	13.1 ± 1.1

The ratio

$$\frac{0.94}{13.1} = 0.072 \pm 13\%$$

leads to the mean free path for absorption in air of

$$L = 125 \pm 8 \text{ gm/cm}^2$$

This is in excellent agreement with the results of photographic plate studies conducted by J. J. Lord.

VIII

COMPARISON WITH OTHER EXPERIMENTAL RESULTS

Positive Excess

Extension of M. Correll's Result

M. Correll (38) found the positive excess of slow mesons at 3.4 kilometers to be 1. The energy range studied was from 60 Mev to 170 Mev (momentum range 140 to 225 Mev/C). The experimental arrangement was one for which all protons of this momentum would have been eliminated. As noted previously, the present investigation not only confirms this result but extends the momentum for which mesons have a positive excess of 1.0 to about 1.25 Bev/C.

Comparison with the Results of Adams, Anderson, et Al

Two separate assumptions will be made here. First, that the meson spectrum has approximately the same form at 30,000 feet as it has at 3.4 kilometers although multiplied by 2.3 from Rossi's (1) curve, and that the proton spectrum has approximately the same form at the two altitudes and is multiplied by the ratio of the "N" component intensities. In view of the similarity of the meson spectra between 3.4 kilometers and sea level found by Potter (37) and the similarity of the proton spectra at 3.4 kilometers and at sea level found

in this study, it is fairly reasonable that this assumption is valid.

Rossi's (1) curve gives a factor of 2.3 in the fast meson rate between 3.4 kilometers and 30,000 feet. The "N" component, however, is multiplied by 14. As 20 per cent of the penetrating component at 3.4 kilometers is protonic, it follows that the expected positive excess at 30,000 feet should be approximately 2.4, which is in excellent, although probably fortuitous, agreement with the results of Adams, Anderson, et al (36), who found a positive excess of 2.5.

The present section is quite speculative in nature, resting on assumptions which are rather insecure. The nice agreement does give considerable support to these assumptions.

Comparison of Momentum Spectra

Comparison with the Results of Goldwasser and Merkle

In order to clarify the comparison of the results of this experiment with that of Goldwasser and Merkle (32) the philosophy of the two experiments will be briefly reviewed. The present experiment was set up, as previously noted, to answer the question: What is the momentum spectrum of those non-electronic particles which have residual ranges (after passing through about 3-1/2 centimeters of lead equivalent) between 0.5 and 10.5 centimeters of lead? The resultant

spectrum separates the protons of this range from the mesons. An approximate picture of the entire momentum spectrum above 0.75 Bev/c can be inferred from these data due to nuclear interactions. The momentum below 0.75 Bev/c is, however, not made available by this experiment. In order to make any comparison with the results of Merkle and Goldwasser it is necessary to assume a proton spectrum below 0.75 Bev/c, which seems reasonable in comparison with the spectrum at higher momenta. When this is done it is found possible to make estimates of the number of protons stopping in a range from 0 to 10 centimeters. The meson spectrum, because of its approach to zero and because of the extreme penetrating power of mu mesons, is little affected by 1/2 centimeter of lead.

The experiment of Goldwasser and Merkle is designed to answer a different question. Here the question asked is this: What is the mass of a particle that has a residual range between 0 and 10 centimeters of copper (approximately 9 centimeters of lead)? By counting the number of particles that have mesonic mass and those that have protonic mass that stop in the copper in a given time one point on the differential range spectrum of protons and one on the spectrum of mesons is determined. Varying the amount of lead above the system provided the entire differential range spectrum. It

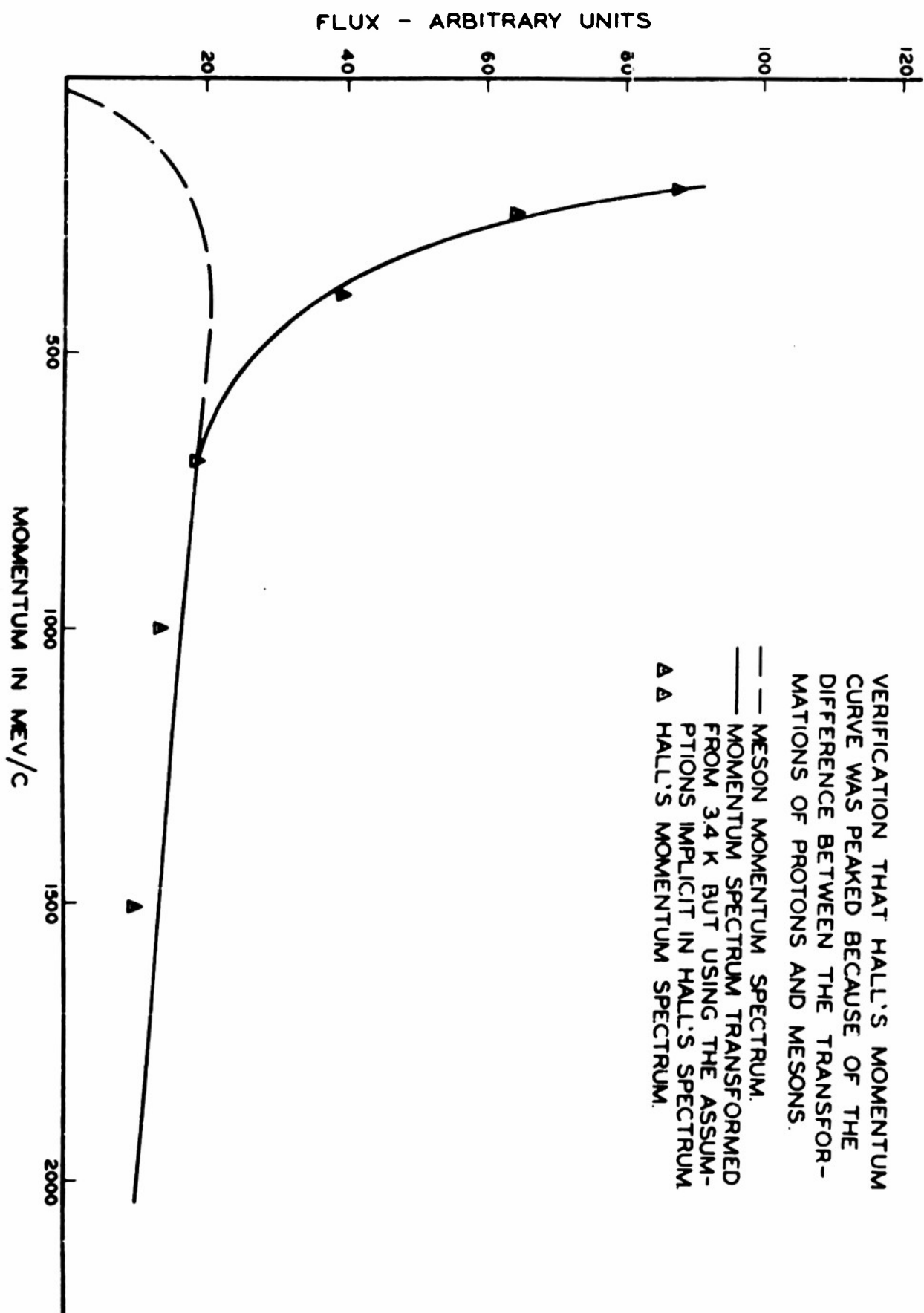
should be noted that the measurement includes particles of all momenta provided they have arrived in the range chamber and that their range does not exceed 10 centimeters of copper. The two experiments in many ways are mutually exclusive as the range spectrum for protons cannot be made to yield the momentum spectrum due to the large number of high momentum protons that stop because of nuclear collisions. On the other hand, it is only by insisting on a minimum range that a momentum spectrum can be made to give information about the relative numbers of mesons and protons.

In view of the necessity of extrapolating the momentum spectrum, it appears that an attempt to make a close comparison between the two experiments is inadvisable although a qualitative agreement on the ratio of protons to mesons apparently exists.

Comparison with Results of Hall

The momentum spectrum obtained by Hall (35) at 4.3 kilometers had a very high peak at about .2 Bev/C. It was noted in the introduction that the form of this spectrum was probably influenced by a large number of protons in the cosmic radiation. It is easy to show that such a hypothesis leads to a spectrum that is very similar to the one obtained by Hall. Several assumptions must be made but the plausibility of them has already been shown in other sections.

The principal assumption is that the proton and meson spectra at 4.3 kilometers have the same form as at 3.4 kilometers. The proton flux at 4.3 kilometers, however, may be estimated from the mean free path of the "N" component in the air - 125 grams per square centimeter. The mass of the air layer between 3.4 and 4.3 kilometers is 85 grams per square centimeter and therefore the proton intensity at 4.3 kilometers is 2.0 times the intensity at 3.4 kilometers. Using the meson range momentum spectrum, and taking account of the nuclear collision processes, a momentum spectrum which corresponds to the momentum spectrum given by Hall was computed. The remarkable similarity of the two curves is shown by Fig. 20. The dropping of Hall's curve below 200 Mev/C is an unavoidable instrumental effect. The curves were normalized at 700 Mev/C. The increasing peaking of the meson spectra towards the lower momenta has not been taken into account here. If this effect were taken into account the rather small discrepancies would be reduced. The momentum spectrum computed in this section is not the one that would be found at 4.3 kilometers but rather is the result of an attempt to duplicate Hall's derived momentum spectrum.



VERIFICATION THAT HALL'S MOMENTUM CURVE WAS PEAKED BECAUSE OF THE DIFFERENCE BETWEEN THE TRANSFORMATIONS OF PROTONS AND MESONS.

IX

SUMMARY

1. The momentum spectrum of protons between 0.75 Bev/C and 2 Bev/C at 3.4 kilometers has been derived from the momentum spectrum of particles stopping in given range intervals. The flux of protons is about half as large as the negative meson flux.

2. The momentum spectrum of protons in the same momentum interval at sea level has been found. The proton flux is about 5 per cent of the total meson flux.

3. A momentum spectrum for mesons alone has been derived from the data of Miller, Henderson, et al by subtracting the proton flux from the positive meson spectrum. The spectra of positive and negative mesons are equal up to 1.25 Bev/C momentum. Above this point the positive excess is greater than one.

4. The proton flux has been correlated to the "N" component of Rossi and the intensity of protons in the momentum interval measured found to be proportional to the "N" component. The mean free path in air of this "N" component has been found to be 132 grams per square centimeter, in good agreement with J. J. Lord and other investigators. This value was obtained in the comparison of

intensities between 3.4 kilometers and sea level; and also between 3.4 kilometers and 30,000 feet.

5. Definite indications that the peak in the momentum spectrum Hall obtained at 4.3 kilometers was due to large numbers of protons in the cosmic radiation have been presented.

6. The mean free path for removal of protons in lead has been shown to be 174 ± 30 grams per square centimeter which agrees, within the statistical uncertainties of measurement, with the 156 to 165 grams per square centimeter of Walker, Walker, and Greisen, J. J. Lord, and others.

BIBLIOGRAPHY

1. Rossi, B. Rev. Mod. Phys., 20:537 (1948).
2. Bhabha, H. J., and Heitler, W. Proc. Roy. Soc., 159:432 (1937).
3. Carlson, J. F., and Oppenheimer, J. R. Phys. Rev., 51:220 (1937).
- 4a. Arley, N. Proc. Roy. Soc., 168:519 (1938).
- b. ———, Stochastic Processes and Cosmic Radiation.
Copenhagen: G. E. C. Gads Forlag, 1943.
5. Rossi, B., and Greisen, K. Rev. Mod. Phys., 13:240 (1941).
6. Bridge, H. Phys. Rev., 72:172 (1947).
7. Bridge, H., Hazen, W. E., Rossi, B., and Williams, R. W. Phys. Rev., 74:1083 (1948).
8. Bridge, H., and Rossi, B. Phys. Rev., 71:379 (1947).
9. Kulsizer, R. I. Phys. Rev., 73:1252 (1948).
10. McClure, G. W., and Pomerantz, M. A. Phys. Rev., 79:911 (1950).
11. Whyte, G. N. Phys. Rev., 82:204 (1951).
12. Anderson, C. D., and Neddermeyer, S. H. Phys. Rev., 50:263 (1936).
13. Brode, R. B., Macpherson, H. G., and Starr, M. A. Phys. Rev., 50:581 (1936).
14. Fussell, H. Phys. Rev., 51:1005 (1936).
15. Powell, W. M. Phys. Rev., 69:385 (1946).
16. Hazen, W. E. Phys. Rev., 65:67 (1944).

17. Cool, R. L., Fowler, E. G., et al. Phys. Rev., 75:1275 (1949).
18. Valley, G. E., Leavitt, C. P., and Vitale, J. A. Phys. Rev., 75:201 (1949).
- 19a. Greisen, K., Walker, W. D., and Walker, S. F. Phys. Rev., 80:535 (1950).
- b. Walker, W. D., Walker, S. F., and Greisen, K. Phys. Rev., 80:546 (1950).
20. Blau, M., and Wambacher, H. Akad. Wiss. Wein IIA 146:623 (1937).
21. Stetter, G., and Wambacher, H. Physik. Zeits., 40:702 (1939).
22. Pickup, E., and Voyvodic, L. Phys. Rev., 82:265 (1951).
23. Camerini, V., Fowler, P. H., Lock, W. O., and Muirhead, H. Phil. Mag., 41:413 (1950).
24. Lord, J. J., Fainberg, J., and Schein, M. Phys. Rev., 80:970 (1950).
25. Lord, J. J. Phys. Rev., 81:901 (1951).
26. Wilson, J. G. Nature, 158:414 (1946).
27. Hughes, D. J. Phys. Rev., 57:597 (1940).
28. Blackett, P. M. S. Proc. Roy. Soc., A159:1 (1937).
29. Glaser, D. A., Hamermesh, B., and Safonov, C. Phys. Rev., 80:625 (1950).
30. Williams, E. J. Proc. Roy. Soc. A172:194 (1939).
31. Merkle, T. C., Jr., Goldwasser, E. L., and Brode, R. B. Phys. Rev., 79:926 (1950).
32. Goldwasser, E. L., and Merkle, T. C., Jr. Phys. Rev., 83:43 (1951).
33. Nonnemaker, G. M., and Street, J. C. Phys. Rev., 82:564 (1951).

34. Miller, C. E., Henderson, J. E., et al. Phys. Rev., 79:459 (1950).
35. Hall, D. B. Phys. Rev., 66:321 (1944).
36. Adams, R. V., Anderson, C. D., et al. Rev. Mod. Phys., 20:334 (1948).
37. Potter, D. S. "The Momentum Spectrum of Cosmic Rays at 3.4 Kilometers." A doctoral thesis, University of Washington, 1951.
38. Correll, M. Phys. Rev., 72:1054 (1947).
39. Gross, E. P., as noted in Montgomery, D. J. X., Cosmic Ray Physics. Princeton: Princeton University Press, 1949, pp. 349-357.
40. Handbook of Chemistry and Physics. Dayton, Ohio: Chemical Rubber Publishing Company.

DISTRIBUTION LIST

Professional

Dr. W. F. G. Swann, Director
Bartol Research Foundation
Franklin Institute
Swarthmore, Pennsylvania

Prof. C. C. Lauritsen
Department of Physics
California Institute of Technology
Pasadena, California

Prof. C. D. Anderson
Department of Physics
California Institute of Technology
Pasadena, California

Prof. R. B. Brode
Department of Physics
University of California
Berkeley 4, California

Prof. E. O. Lawrence
Radiation Laboratory
University of California
Berkeley 4, California

Prof. J. R. Richardson
Department of Physics
University of California
(Los Angeles)
Los Angeles 24, California

Prof. E. C. Creutz
Department of Physics
Carnegie Institute of Technology
Schenley Park
Pittsburgh 13, Pennsylvania

Dr. M. A. Tuve
Department of Terrestrial Magnetism
Carnegie Institution of Washington
Washington, D. C.

Dr. R. S. Shankland
Case Institute of Technology
Department of Physics
University Circle
Cleveland 6, Ohio

Prof. S. K. Allison
Institute of Nuclear Studies
University of Chicago
Chicago, Illinois

Prof. J. Rainwater
Columbia University
Nevis Cyclotron Laboratories
P. O. Box 117
Irvington-on-Hudson, New York

Prof. R. R. Wilson
Laboratory of Nuclear Studies
Cornell University
Ithaca, New York

Prof. W. M. Nielson
Department of Physics
Duke University
Durham, North Carolina

Dr. Guy Suits
Research Laboratory
General Electric Company
Schenectady, New York

Dr. Zoltan Bay
Department of Physics
George Washington University
Washington, D. C.

Prof. N. F. Ramsey
Department of Physics
Harvard University
Cambridge, Massachusetts

Director
Nuclear Laboratory
Harvard University
Cambridge, Massachusetts

Prof. F. W. Loomis
Department of Physics
University of Illinois
Urbana, Illinois

Prof. A. C. G. Mitchell
Department of Physics
Indiana University
Bloomington, Indiana

Prof. J. A. Van Allen
Department of Physics
State University of Iowa
Iowa City, Iowa

Prof. J. D. Stranathan
Department of Physics
University of Kansas
Lawrence, Kansas

Prof. J. M. Cork
Department of Physics
University of Michigan
Ann Arbor, Michigan

Prof. W. E. Hazen
Department of Physics
University of Michigan
Ann Arbor, Michigan

Prof. C. E. Williams
Department of Physics
University of Minnesota
Minneapolis, Minnesota

Prof. E. P. Ney
Department of Physics
University of Minnesota
Minneapolis, Minnesota

Prof. Truman S. Gray
Serve-Mechanisms Laboratory
Massachusetts Institute of Technology
Cambridge 39, Massachusetts

Professor J. R. Zacharias. . . . (2)
Laboratory for Nuclear Science and
Engineering
Massachusetts Institute of Technology
Cambridge 39, Massachusetts

Prof. S. A. Korff
Department of Physics
New York University
University Heights
New York 53, New York

Prof. E. Waldman
Nuclear Physics Laboratory
University of Notre Dame
Notre Dame, Indiana

Prof. J. N. Cooper
Department of Physics
Ohio State University
Columbus 10, Ohio

Prof. W. E. Stephens
Department of Physics
University of Pennsylvania
Philadelphia 4, Pennsylvania

2 Prof. A. J. Allen
Department of Physics
University of Pittsburgh
Pittsburgh, Pennsylvania

Prof. G. T. Reynolds
Department of Physics
Princeton University
Princeton, New Jersey

Prof. M. G. White
Department of Physics
Princeton University
Princeton, New Jersey

Prof. Leticia del Rosario
Department of Physics
Gobierno De Puerto Rico
Universidad De Puerto Rico
Rio Piedras
Puerto Rico

Prof. K. Lark-Horovitz
Department of Physics
Purdue University
Lafayette, Indiana

Prof. T. W. Bonner
Department of Physics
Rice Institute
Houston, Texas

Prof. R. E. Marshak
Department of Physics
University of Rochester
Rochester, New York

Prof. Charles A. Whitmer
Chairman, Department of Physics
Rutgers University
New Brunswick, New Jersey

Prof. E. L. Ginzton
Microwave Laboratory
Stanford University
Palo Alto, California

Prof. F. Bloch
Department of Physics
Stanford University
Palo Alto, California

Prof. J. D. Trimmer
Department of Physics
University of Tennessee
Knoxville, Tennessee

Prof. A. L. Hughes
Department of Physics
Washington University
St. Louis, Missouri

Prof. R. D. Sard
Department of Physics
Washington University
St. Louis, Missouri

Prof. J. H. Manley
Department of Physics
University of Washington
Seattle 5, Washington

Mr. J. W. Coltman
Research Laboratories
Westinghouse Electric Corporation
East Pittsburgh, Pennsylvania

Prof. R. L. Herb
Department of Physics
University of Wisconsin
Madison 6, Wisconsin

Prof. W. W. Watson (2)
Department of Physics
Sloane Physics Laboratory
Yale University
New Haven, Connecticut

Governmental

Chief of Naval Research (2)
Attn: Nuclear Physics Branch
Navy Department
Washington 25, D. C.

Director, Naval Research Laboratory (9)
Attn: Technical Information Officer
Washington 25, D. C.

Director
Office of Naval Research
Chicago Branch Office
844 North Rush Street
Chicago 11, Illinois

Director
Office of Naval Research
San Francisco Branch Office
801 Donahue Street
San Francisco 24, California

Director
Office of Naval Research
New York Branch Office
346 Broadway
New York 13, New York

Director
Office of Naval Research
Pasadena Branch Office
1030 East Green Street
Pasadena 1, California

Officer in Charge (10)
Office of Naval Research
Navy No. 100
Fleet Post Office
New York, New York

Superintendent, Nucleonics Division
Naval Research Laboratory
Anacostia, Washington, D. C.

Chief, Bureau of Ships
Attn: Code 390
Navy Department
Washington 25, D. C.

Chief, Bureau of Ships
Attn: Code 330
Navy Department
Washington 25, D. C.

Chief, Bureau of Ordnance
Attn: Rem
Navy Department
Washington 25, D. C.

Chief, Bureau of Ordnance
Attn: Re9a
Navy Department
Washington 25, D. C.

Chief, Bureau of Aeronautics
Attn: RS-5
Navy Department
Washington 25, D. C.

Chief, Bureau of Aeronautics
Attn: Technical Library
Navy Department
Washington 25, D. C.

Commanding Officer
Naval Radiological Defense Laboratory
San Francisco Naval Shipyard
San Francisco 24, California

Chief of Naval Operations
Attn: Op 36
Navy Department
Washington 25, D. C.

Commander, U. S. Naval Ordnance Test
Station
Technical Library
Inyokern, China Lake, California

Commanding General
Air Force Cambridge Research Center
Attn: Geophysics Research Library
250 Albany Street
Cambridge 39, Massachusetts

Senior Scientific Advisor
Office of the Under Secretary
of the Army
Department of the Army
Washington 25, D. C.

Director, Research and Development
Division
General Staff
Department of the Army
Washington 25, D. C.

Chief, Physics Branch
U. S. Atomic Energy Commission
1901 Constitution Avenue, N. W.
Washington 25, D. C.

U. S. Atomic Energy Commission
Attn: Roland Anderson
Patent Branch
1901 Constitution Avenue, N. W.
Washington 25, D. C.

U. S. Atomic Energy Commission . . (4)
Library Branch
Technical Information Division, ORE
P. O. Box E
Oak Ridge, Tennessee

Oak Ridge National Laboratory
Attn: Head, Physics Division
P. O. Box P
Oak Ridge, Tennessee

Brookhaven National Laboratory
Attn: Dr. S. C. Stanford
Research Library
Upton, L. I., New York

Oak Ridge National Laboratory
Attn: Central Files
P. O. Box P
Oak Ridge, Tennessee

Argonne National Laboratory
Attn: Hoylande D. Young
P. O. Box 5207
Chicago 80, Illinois

Document Custodian
Los Alamos Scientific Laboratory
P. O. Box 1663
Los Alamos, New Mexico

Technical Information Group
General Electric Company
P. O. Box 100
Richland, Washington

Carbide and Carbon Chemical Division
(K-25 Plant)
Plant Records Department
Central Files (K-25)
P. O. Box P
Oak Ridge, Tennessee

Carbide and Carbon Chemical Division
(Y-12 Plant)
Central Reports & Information (Y-12)
P. O. Box P
Oak Ridge Tennessee

Ames Laboratory
Iowa State College
P. O. Box 14A, Station A
Ames, Iowa

Knolls Atomic Power Laboratory
Attn: Document Librarian
P. O. Box 1072
Schenectady, New York

Mound Laboratory
Attn: Dr. M. M. Haring
U. S. Atomic Energy Commission
P. O. Box 32
Miamisburg, Ohio

Sandia Corporation
Sandia Base
Attn: Mr. Dale N. Evans
Classified Document Division
Albuquerque, New Mexico

U. S. Atomic Energy Commission
Attn: Division of Technical Information
and Declassification Service
New York Operations Office
P. O. Box 30
Arsonia Station
New York 23, New York

National Bureau of Standards Library
Room 203, Northwest Building
Washington 25, D. C.

Director, Office of Ordnance Research
2127 Myrtle Drive
Durham, North Carolina

National Science Foundation
2144 California Street
Washington 25, D. C.

Director
Office of Naval Research
Boston Branch Office
150 Causeway Street
Boston, Massachusetts

Commanding General
Air Research & Development Command
Attn: RDRRF
P. O. Box 1359
Baltimore 3, Maryland

Foreign

Doctor Cesar Lattes
Scientific Director, Brazilian Center
of Physical Research
Rio de Janeiro, Brazil